

# The anterior commissure is a pathway for contralateral spread of herpes simplex virus type 1 after olfactory tract infection

Eva Jennische · Charlotta E. Eriksson · Stefan Lange · Edward Trybala · Tomas Bergström

Received: 3 October 2014 / Revised: 22 December 2014 / Accepted: 26 December 2014 / Published online: 21 January 2015  
© Journal of NeuroVirology, Inc. 2015

**Abstract** Herpes simplex encephalitis (HSE), targeting the limbic system, is the most common cause of viral encephalitis in the Western world. Two pathways for viral entry to the central nervous system (CNS) in HSE have been suggested: either via the trigeminal nerve or via the olfactory tract. This question remains unsettled, and studies of viral spread between the two brain hemispheres are scarce. Here, we investigated the olfactory infection as a model of infection and tropism of herpes simplex virus 1 (HSV-1), the causative agent of HSE, in the CNS of rats. Rats were instilled with HSV-1 in the right nostril and sacrificed 1–6 days post-infection, and tissues were analysed for viral spread using immunohistochemistry and quantitative PCR (qPCR). After nasal instillation, HSV-1 infected mitral cells of the olfactory bulb (OB) on the right side only, followed by limbic encephalitis. As a novel finding, the anterior commissure (AC) conveyed a rapid transmission of virus between the right and the left OB, acting as a shortcut also between the olfactory cortices. The neuronal cell population that conveyed the viral infection via the AC was positive for the water channel protein aquaporin 9 (AQP9) by immunohistochemistry. Quantification of AQP9

in cerebrospinal fluid samples of HSE patients showed increment as compared to controls. We conclude that the olfactory route and the AC are important for the spread of HSV-1 within the olfactory/limbic system of rats and furthermore, we suggest that AQP9 is involved in viral tropism and pathogenesis of HSE.

**Keywords** Herpes simplex virus type 1 · Herpes simplex encephalitis · Olfactory bulb · Anterior commissure · Oligodendrocytes · Aquaporin 9

## Introduction

Herpes simplex encephalitis (HSE) is acknowledged as the most common cause of viral encephalitis in the Western world, responsible for up to 20 % of the cases (Granerod et al. 2011; Hjalmarsson et al. 2007; Steiner 2011). Affecting 2–4 inhabitants per million people per year (Hjalmarsson et al. 2007; Whitley 2006), HSE can be caused by either primary or recurrent infection of herpes simplex virus type 1 (HSV-1) (Steiner 2011; Whitley et al. 1982). Brain infection resulting in HSE has been suggested to occur after viral invasion via the trigeminal nerve (Davis and Johnson 1979), the olfactory tract (Esiri 1982) or via both routes (Esiri and Tomlinson 1984; Nagashima et al. 1998). It has been reported that in early stages of HSE, abundance of HSV-1 antigen in the olfactory bulb (OB) and tract might be related to the final location of inflammation and necrosis in the central nervous system (CNS) (Esiri 1982). In addition, the viral spread within the brain and between the two brain hemispheres has been less extensively examined, but is most likely decisive for location and development of clinical manifestations of HSE.

---

E. Jennische and C. E. Eriksson have contributed equally to this work.

**Electronic supplementary material** The online version of this article (doi:10.1007/s13365-014-0312-0) contains supplementary material, which is available to authorized users.

E. Jennische  
Department of Medical Biochemistry and Cell Biology, Institute of Biomedicine, University of Gothenburg, Gothenburg, Sweden

C. E. Eriksson · S. Lange · E. Trybala · T. Bergström (✉)  
Department of Infectious Diseases, Institute of Biomedicine, University of Gothenburg, Gothenburg, Sweden  
e-mail: tomas.bergstrom@microbio.gu.se

Prior to the introduction of the nucleoside analogue drug acyclovir, the mortality rate in HSE patients was over 70 % (Kennedy and Chaudhuri 2002), but with antiviral treatment, the mortality rate has markedly decreased to around 10–30 % (Riancho et al. 2013; Skoldenberg et al. 1984; Steiner 2011; Whitley et al. 1986). Between 25 and 90 % of the surviving patients treated with antiviral therapy have been reported to present with neurological sequelae (Hjalmarsson et al. 2007; McGrath et al. 1997; Moon et al. 2014; Raschilas et al. 2002; Sili et al. 2014; Stahl et al. 2012; Whitley 2006) while for untreated survivors, the corresponding number is around 90 % (Whitley 2006). The most commonly described rest conditions are epilepsy, dysphasia, amnesia and behavioural disturbances (Hjalmarsson et al. 2007; Misra et al. 2008; Riancho et al. 2013). Better knowledge of the viral spread could result in target medication which in turn could decrease the occurrence of neurological sequelae in surviving HSE patients.

In rodent models, viral spread of HSE via the olfactory tract in mice and rats has been observed to extend from the nasal cavity into the CNS (Mori et al. 2005). The olfactory receptor neuron passes through the olfactory epithelium, penetrates the cribriform plate and enters the OB to reach CNS. In the OB, the olfactory receptor neurons connect in glomeruli to mitral cells (second-order neurons), which in turn project to the olfactory system and the limbic system (Mori et al. 2005). The limbic system, which involves amygdala, hippocampus and the OBs, is evolutionary one of the oldest parts of the brain, and it has been suggested that the clinical manifestations of HSE are due to a special affinity to the limbic cortices for HSV-1 as HSE cause selective damage to the grey matter of the entire limbic system (Damasio and Van Hoesen 1985). Hence, HSV-1 may find its way from the OB through the brain using evolutionary conserved routes.

HSE is characterized by focal findings such as hemiparesis, focal seizures and autonomic dysfunctions associated with damage of the inferior parts of the temporal lobe (Hudson et al. 1991; Kennedy and Steiner 2013; Whitley 2006). These findings are reflected by the clinical manifestations of HSE seen both in magnetic resonance imaging (MRI) (De Tiege et al. 2008; Oyanguren et al. 2013) and through autopsy investigations of HSE-affected brain (Davis and Johnson 1979; Esiri 1982). Although there are numerous descriptive studies of the clinical manifestations, the understanding of the underlying viral pathogenetic mechanisms is lacking. The use of neurotropic viruses as neuronal tracers is considered to be one way of elucidation (Norgren and Lehman 1998). Because of its spread in CNS, HSV-1, along with other viruses, has been suggested for use as a neuronal tracer to examine neural circuits to determine their function (Kristensson et al. 1982; Kuypers and Ugolini 1990; Norgren and Lehman 1998; Turner and Jenkins 1997).

In this study, we have investigated the spread of HSV-1 in rat brain after intranasal instillation of virus in the right nostril. Our results indicate an early spread to the right trigeminal ganglion (TG) and right OB followed by a later infection of the same structures on the contralateral side, i.e. that both the trigeminal and olfactory routes were utilized. Interestingly, the spread between the two OBs was mediated via the anterior commissure (AC). Furthermore, HSV-1 antigen-positive cells in this neuronal tract were co-stained for aquaporin 9 (AQP9). This led us to investigate the concentration of AQP9 protein in human serum and cerebrospinal fluid (CSF) and RNA expression of AQP9 in rat brain tissues. We found a statistically significant increase in AQP9 concentration for HSE patients compared with controls, which suggests that AQP9 expression is upregulated during human HSV-1 infection of the brain.

## Material and methods

### Virus

HSV-1 2762, a clinical isolate from a brain biopsy of a 58-year-old male patient who presented with focal encephalitis which later turned out to be fatal (Bergstrom et al. 1990), was used for infection of rats. The virus has been shown to be highly neurovirulent in animal models (Bergstrom et al. 1990). Isolation of the virus from the brain biopsy was approved in 1981 by the ethics committees at the universities of Gothenburg, Linköping, Lund, Umeå and Uppsala at the Karolinska Institute, for a Swedish multicentre study on antiviral treatment in HSE (Skoldenberg et al. 1984) conducted according to the principles expressed in the Helsinki declaration. Virus stocks of HSV-1 strain 2762 were prepared from low passages.

### Animals

Male Sprague–Dawley (SD) rats, body weight  $250 \pm 20$  g, (Harlan Laboratories, Boxmeer, The Netherlands) were used (infected rats  $n=49$ , control rats  $n=11$ ). The regional Ethical Committee on Animal Experiments approved the test protocol, and all experiments were performed in accordance with the EC Directive 86/609/EEC guidelines for animal experiments. The rats were allowed a week for general adaptation before the start of the experiments, and they had constantly free access to pelleted food and water. The temperature and air ventilation in the animal quarters were monitored according to standard procedures; a 12-h light cycle was used and the air was exchanged 17 times per hour.

### Human samples for measurement of AQP9 concentration

Possible subjects were included in the study preferably if samples of both CSF and serum were available, and these samples should have been taken within a week of each other.

From the Regional Biobank Centre at Sahlgrenska University Hospital in Gothenburg, samples were obtained from patients with HSE ( $n=23$ ) diagnosed through positive quantitative PCR (qPCR) results for HSV-1 in CSF (Namvar et al. 2005), where the inclusion criteria was a value equal to or higher than 1000 genome equivalents/ml (geq/ml). The statements related to the PCR results for HSE determination were noted, and samples were excluded if other parallel diagnoses were suspected. For 8 of these patients, only CSF samples were available, but these were nevertheless included in the analysis. Controls samples ( $n=19$ ) had previously been obtained from healthy subjects. The mean age and the gender distribution between the healthy controls and the HSE patients differed, but as withdrawal of CSF samples is ethically hard to motivate, these were the samples available. For HSE patients, the mean age was 62.7 years (age span 27–87 years), and for healthy controls, the mean age was 33.3 years (age span 18–56 years). Both male and female subjects were included with a slight female overweight for HSE samples ( $n=11$ ) and a male overweight for healthy subjects ( $n=16$ ).

Six HSE patients contributed with more than one sample, taken at different time points during the infection, and these were therefore analysed separately from the two groups in order to investigate the level of AQP9 during convalescence.

Experiments were conducted with approval from the Regional Research Ethics Committee in Gothenburg in accordance with the Declaration of Helsinki and local regulations.

### Infection by intranasal instillation of HSV-1

The encephalitogenic infection in rats was achieved after intranasal instillation in the right nostril with HSV-1, with a volume of 25  $\mu$ l (total dose given= $1.1 \times 10^4$  plaque forming units (pfu)), as described previously (Jennische et al. 2008). This instillation was adapted from an inoculation method described by RT Johnson (Johnson 1964). The infective dose was always placed in the right nostril while the rat was under deep isoflurane (Forane, Baxter, Deerfield, IL) anaesthesia. The rats were sacrificed day 1 ( $n=5$ ), 2 ( $n=5$ ), 3 ( $n=10$ ), 4 ( $n=10$ ), 5 ( $n=14$ ) and 6 ( $n=5$ ) post-infection. For ethical reasons, the extent of the experiment could not exceed day 6 p.i., as all animals by then were symptomatic.

Animals showing definitive symptoms of neurological dysfunction and signs associated with focal inflammation, i.e. repetitive, stereotypic movements, rotational vertigo and motor instability, were immediately euthanized. The decision to sacrifice the neurologically affected animals

was taken by the researchers or by a skilled animal technician.

### DNA extraction

Rats whose tissues were to be used in real-time qPCR for DNA quantification of HSV-1 were sacrificed day 1, 2, 3, 4 and 5 p.i. The brain was surgically removed from the sacrificed rats, separating tissues from each other and storing them in freezer at  $-80$  °C until use. The tissues of special interest were the OBs (left and right), the TGs (left and right), hippocampus (left and right), lamina cribrosa and the brain stem.

To obtain homogenized samples, 2–3 pieces from the tissue of interest (approximately 10–20 mg in size) were added to a tube containing MagNA Lyser Green Beads (Roche Diagnostics, Mannheim, Germany) along with MagNA Pure 96 DNA Tissue Lysis Buffer (Roche). A homogenizing step was performed using a MagNA Lyser instrument (Roche) for 2 runs at 6500 rpm of 45 s each. The homogenized samples were treated with proteinase K for 30 min at 55 °C and were then subjected for centrifugation at  $16,000 \times g$  for 2 min. The resulting supernatants were then obtained and stored at  $-80$  °C.

Using a MagNA Pure LC DNA Isolation Kit II Tissue (Roche) according to the manufacturer's instructions, the homogenized samples were subjected to DNA purification in a MagNA Pure LC robot (Roche).

### RNA extraction

For RNA quantification of rat AQP9 and internal control 18S, HSV-1-infected rats 5 days p.i. ( $n=4$ ) and control rats ( $n=2$ ) were sacrificed. Tissues of interest (left and right OB, left and right hippocampus and left and right AC area) were surgically removed from sacrificed rats and stored at  $-80$  °C until homogenization. For homogenization, small pieces from the tissue of interest (around 30–70 mg) were added to a tube containing MagNA Lyser Green Beads (Roche) along with 1 ml of QIAzol Lysis Reagent (QIAGEN Nordic, Sollentuna, Sweden). A MagNA Lyser instrument (Roche) was operated at 5000 rpm for 80 s, and the lysate was transferred to a new tube and stored at  $-80$  °C until RNA purification. Using the RNeasy Lipid Tissue Mini Kit (QIAGEN), the homogenized samples were isolated for total RNA to a final eluted volume of 100  $\mu$ l. The procedures were performed according to the QIAGEN protocol 'Purification of total RNA using the RNeasy Lipid Tissue Mini Kit' step 4–16, with inclusion of a step for on-column DNase digestion with the RNase-Free DNase Set (QIAGEN). The concentration and purity of the RNA preparations was controlled using spectrophotometry, by the 260/280 nm absorbance ratio (mean  $2.04 \pm SD$  0.056).

## Real-time quantitative PCR

The qPCR for DNA quantification was performed as described previously (Namvar et al. 2005). Amplification of the glycoprotein B (gB) region of HSV-1 was performed using 7300 Real-Time PCR System (Applied Biosystems, Foster City, CA) with a pair of primers (forward HSV-1 5' GCAGTTTACGTACAACCACATACAGC'3 and reverse HSV-1 3'AGCTTGCGGGCCTCGTT'5) and an HSV-1 gB-specific probe (5'CGGCCCAACATATCGTTGACATGGC'3) labelled with 6-carboxyfluorescein (FAM) and 6-carboxytetramethyl-rhodamine (TAMRA). This resulted in detection and amplification of a 118-nucleotide segment of the highly conserved gB-region of HSV-1, giving a specific cycle threshold ( $C_t$ ) value which was recorded. The  $C_t$ -value was defined as the number of PCR cycles required for the fluorescent signal to exceed the threshold value. By relating the detected  $C_t$ -values to a standard curve, the number of HSV-1 DNA copies in each sample was determined.

For RNA quantification, commercially pre-developed TaqMan Gene Expression Assays™ (Applied Biosystems, Life Technologies Europe, Stockholm, Sweden) were purchased. The assay for rat AQP9 (Rn00576331\_m1), with the probe sequence TTTGAGGTCTTCACAGTTGGAAATA, had the probe spanning across an exon, while for the internal control rat 18S (Rn03928990\_g1) to detect genomic DNA, the probe TACTTGGATAACTGTGGTAATTCTA as well as the primer sequences were mapped within a single exon. The probes were fluorescently labelled with FAM in their 5' end and quenched in the 3' end. RNA analysis of samples was performed using the SuperScript III One-Step RT-PCR System (Invitrogen, Life Technologies Europe, Stockholm, Sweden), where 12.5  $\mu$ l of Reaction Mix (Invitrogen), 0.5  $\mu$ l of SuperScript III RT/Platinum TaqMix (Invitrogen), 9.25  $\mu$ l of RNase-Free Water (Sigma-Aldrich, St. Louis, MO), 0.5  $\mu$ l of RNase OUT (Invitrogen) and 1.25  $\mu$ l of the Gene Expression Assay was added to wells of 96-well plates along with 40 ng/ $\mu$ l (for AQP9) or 4 pg/ $\mu$ l (for 18S) of total RNA. A total of 25  $\mu$ l of reaction volume was added per well, and all qPCR reactions were performed in triplicates. Amplification was performed using 7300 Real-Time PCR System (Applied Biosystems) with a reverse transcriptase reaction step performed at 48 °C for 30 min, followed by a polymerase activation step at 95 °C for 10 min and a PCR cycle (95 °C for 15 s, 60 °C for 1 min) for 45 cycles in total. 18S, which is a house-keeping gene previously shown to be constantly expressed in herpesvirus-infected cells (Nyström et al. 2004), was used for normalization of  $C_t$ -values. The standards used in the PCR reactions were plasmids created using CT-GFP Fusion TOPO TA Cloning Kit (Invitrogen) following instructions from the manufacturer and purified using the QIAprep Spin Miniprep Kit (QIAGEN) according to the

manufacturer's instructions. Plasmids were used in 10-fold dilutions in the real-time PCR according to the procedures described above.

## Tissue preparation, histology and immunohistochemistry

Rats for histology investigation, sacrificed day 3, 4, 5 and 6 post-infection, were deeply anesthetized with isoflurane and fixed by transcardial perfusion via the left ventricle with PBS, followed by 4 % formaldehyde. The brains were removed and immersion fixed for about 4 days. The entire brains were then cut into 3–4-mm-thick transversal slices. The slices were dehydrated and embedded in paraffin. In some animals, the skull bases and nasal cavities were decalcified after fixation, using 10 % EDTA in 0.2 M Tris buffer, pH 7.4 for 4–6 weeks and were then embedded in paraffin. Sections were cut at 4  $\mu$ m.

After antigen retrieval, using 0.01 M EDTA in 0.10 M Tris buffer (pH 8.0), the sections were incubated with a polyclonal anti-HSV-1 antibody raised against infected rabbit cornea (B0114, DAKO Denmark A/S, Glostrup, Denmark). Anti-rabbit Impress Reagent HRP (Vector Laboratories, Burlingame, CA) was used as secondary reagent, and the immunoreaction was visualized using liquid DAB+ substrate (DAKO). Nuclei were counterstained with haematoxylin. The sections were then dehydrated and mounted using DPX (Merck Millipore, Darmstadt, Germany). These procedures were performed on sections from both infected and control animals.

To ensure specific HSV-1 staining, control experiments were performed where sections from infected animals (5 days p.i.) were incubated with the solid-phase absorbed control serum Dako Rabbit Immunoglobulin Fraction (Code X0903, DAKO) instead of the polyclonal anti-HSV-1 antibody mentioned above. Same protein concentrations were used for both the polyclonal anti-HSV-1 antibody and the control serum. Haematoxylin were used for counterstaining nuclei.

For double staining experiments, excluding AQP9 double staining, the sections were incubated with the polyclonal HSV-1 antibody previously mentioned along with a monoclonal antibody, either the astrocyte marker GFAP (Novocastra, Newcastle, UK), the microglial marker Iba1 (Santa Cruz Biotechnology, Dallas, TX) or the neuronal nuclei marker NeuN (Chemicon International, Temecula, CA). Cyanine dye 3 (Cy3)-conjugated donkey anti-rabbit IgG (Jackson ImmunoResearch Europe Ltd, Suffolk, UK), and FITC-conjugated donkey anti-mouse IgG (Jackson) were used as secondary reagents. For double staining with HSV-1 and AQP9, a monoclonal HSV-1 antibody (ABIN1020364, antibodies-online GmbH, Aachen, Germany) was used in combination with a polyclonal antibody for AQP9 (Santa Cruz). The Cy3-conjugated donkey anti-rabbit IgG and

Alexa488-conjugated donkey anti-mouse IgG (Jackson ImmunoResearch) were used as secondary reagents. In both cases, nuclei were counterstained with Hoechst blue (Sigma-Aldrich St. Louis, MO) and the sections were mounted in Vectashield (Vector laboratories). A Zeiss Axio Imager M1 microscope (Carl Zeiss AB, Stockholm, Sweden), equipped with Zeiss 5×/0.16 Plan-Apochromat, Zeiss 10×/0.45 Plan-Apochromat, Zeiss 20×/0.80 Plan-Apochromat and Zeiss 40×/0.95 Plan-Apochromat objective lenses, was used for imaging. For documentation, an AxioCAM HRc (Zeiss) was used and acquired images were analysed with AxioVision Rel. 4.8 (Zeiss).

#### Enzyme-linked immunosorbent assay (ELISA)

AQP9 concentrations were measured in human CSF and serum samples using the commercially available ELISA kit SEA578Hu for AQP9 (USCN Life Science Inc., Wuhan, People's Republic of China). Unless otherwise stated, the reagents and chemicals used were provided by the manufacturer.

Following recommendations made by the manufacturer serum samples were diluted 1:10 in PBS pH 7.1. As no recommendations were made for dilution of clinical CSF samples, a test run was performed, deciding that CSF samples were to be diluted 1:5 in PBS pH 7.1.

Diluted samples (serum and CSF) were added in duplicates, along with the provided standard (in 7-fold dilution ranging from 0.156 to 10.0 ng/ml+blank), to an ELISA plate precoated with AQP9-specific antibody according to the manual for the kit (USCN Life Science). The plate was incubated for 2 h at 37 °C. Subsequently, liquid was removed and to each well, a biotin-conjugated antibody specific for AQP9 was added. After 1 h of incubation at 37 °C, washing with wash detergent was performed three times and a secondary unspecific antibody, coupled to Avidin conjugated to horseradish peroxidase (HRP), was added to the wells. For 30 min, the plate was incubated at 37 °C, followed by a 5-fold washing cycle. Addition of 3,3',5,5'-tetramethyl-benzidine (TMB) substrate solution was subsequently performed. The plate was let to incubate for 15 min at 37 °C until change of colour appeared. The reaction was then terminated by addition of the stop solution (solution of sulphuric acid) and the optical density was measured at 450 nm in Multiskan FC (Thermo Scientific, Rockford, IL). By comparing the optical density of the samples to the values of the standard curve, the concentration of AQP9 was determined.

#### Software

Statistical analysis was performed and graphs were constructed using GraphPad Prism version 6.04 (GraphPad Software

Inc., La Jolla, CA). Student's *t* test was used for comparing mean values to calculate *p* value significance. *p* value <0.05 was considered to be statistically significant. Statistics are presented using mean value ± SEM unless otherwise stated.

## Results

### Distribution of HSV-1 spread through quantitative PCR

The distribution of the viral spread in the brain was investigated and illustrated through quantification of the viral DNA in the tissues of interest. The gB-region of the HSV-1 genome was amplified in qPCR with gB-specific primers and probe (Namvar et al. 2005). Tissue samples from the TGs, the OBs, hippocampus, lamina cribrosa and the brainstem were analysed by sacrificing animals from day 1 post-infection (p.i.) (immediate infection) to day 5 p.i. (late infection).

#### *Immediate infection (day 1–2 post-infection)*

On day 1 p.i., only one single animal was HSV-1 DNA positive in the right TG (Fig. 1a) and in lamina cribrosa (a cribriform plate of the ethmoid bone between the olfactory mucosa and the OB (Fig. 1c)). There were no positive signals found anywhere else in the brain, and all other animals showed altogether negative results (Fig. 1). On day 2 p.i., however, all animals presented with HSV-1 DNA in the right TG (Fig. 1a) and a peak in viral load was also observed for most animals in lamina cribrosa (Fig. 1c). Scattered positive results were found in other tissues for single animals at this time point.

#### *Early infection (day 3 post-infection)*

On day 3 p.i., the lamina cribrosa showed a decrement in the viral load (Fig. 1c), while the right TG still showed PCR positivity in all animals (Fig. 1a). Furthermore, HSV-1 DNA was commonly detected in the brainstem (Fig. 1d). While all animals apart from one were negative in the right hippocampus (Fig. 1e), samples from the left hippocampus (Fig. 1f) presented mostly positive results on this time point. Other tissues still only presented scattered positive results.

#### *Late infection (day 4–5 post-infection)*

In late infection, all tissues presented with overall positive findings of HSV-1 DNA. In addition to the tissues which showed positive signals earlier in the infection, the left TG (Fig. 1b), the right hippocampus (Fig. 1e), the right OB

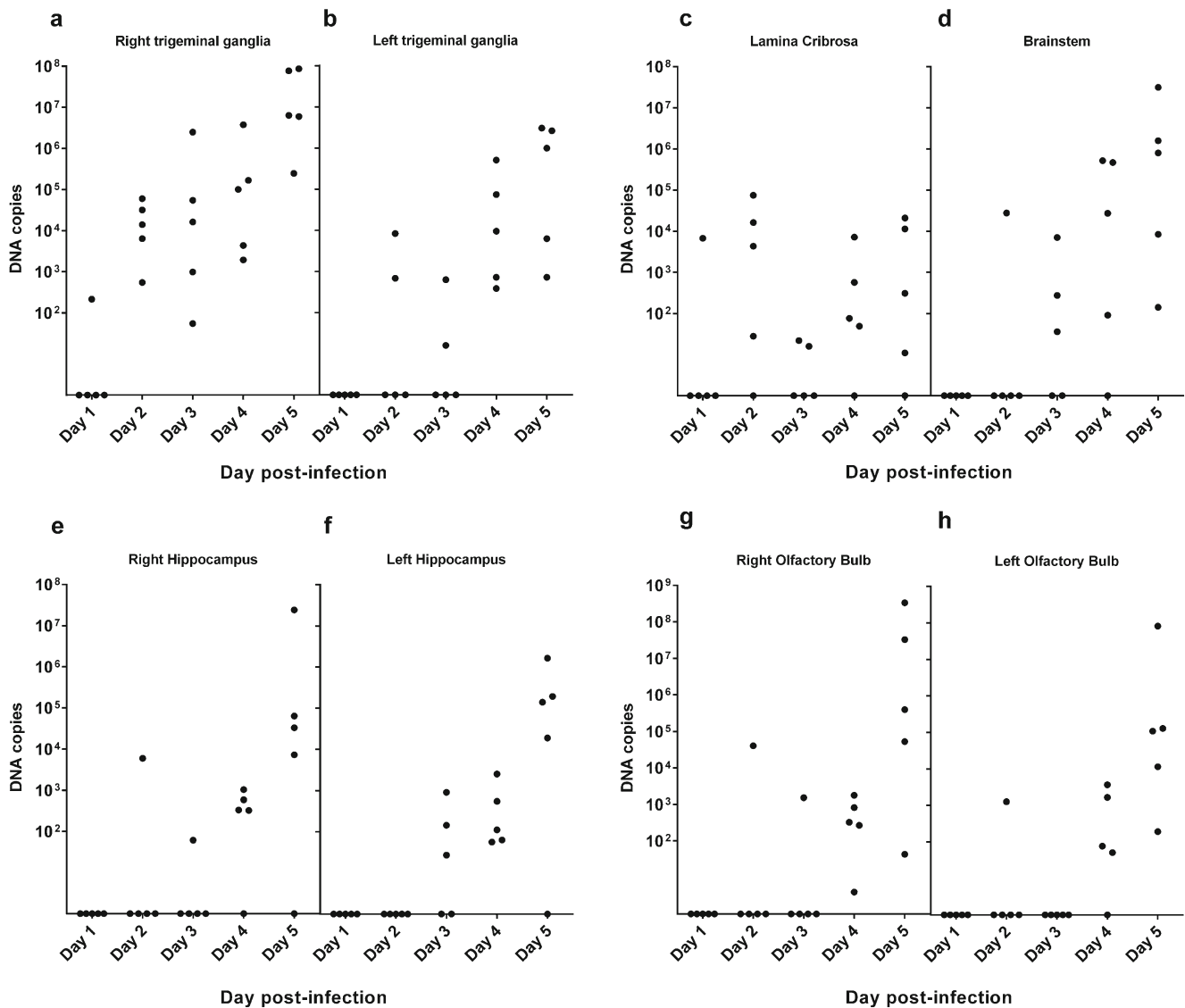


**Fig. 1** HSV-1 DNA quantification for analysis of viral spread 1–5 days after intranasal infection of rat brain. Rats were infected with a neurovirulent strain of HSV-1 through instillation in the right nostril. 1, 2, 3, 4 or 5 days post-infection, rats were sacrificed ( $n=5$  per day) for examination of viral spread to specific brain tissues of interest. The right trigeminal ganglion (**a**) showed positive results for all animals already at day 2 p.i., while overall positive results for HSV-1 in the left trigeminal ganglia (**b**) were delayed until day 4 p.i. The lamina cribrosa (**c**) presented a biphasic pattern of viral presence, with peaks in viral load at day 2 and day

4–5 p.i. For the brain stem (**d**), some animals presented HSV-1 DNA at day 3 p.i., while all animals showed positive signals later in infection. For the right hippocampus (**e**), stronger presentation of HSV-1 DNA was seen day 4 p.i., while the left hippocampus (**f**) showed positive results already day 3 p.i. Positive results for the right olfactory bulb (**g**) were not seen for all animals until day 4 p.i., and there was a slight delay in presentation of HSV-1 DNA for the left olfactory bulb (**h**), where all animals were HSV-1 positive day 5 p.i.

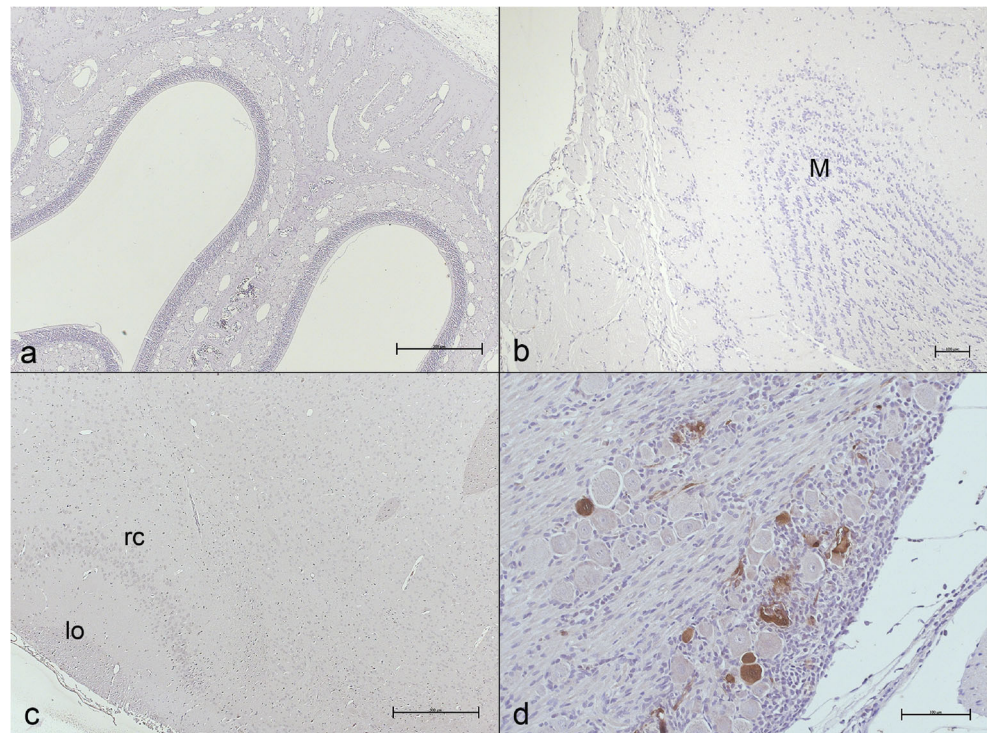
(Fig. 1g) and the left OB (Fig. 1h) all showed positive results. The lamina cribrosa (Fig. 1c) presented a second viral peak, which therefore showed a biphasic pattern in viral load, which could mirror the time frame for viral spread between the right and the left brain hemisphere.

The results from qPCR indicated that there was an almost instant infection of HSV-1 in the right TG, while there was a delay in the spread of the virus to the left TG as shown by day 3, when not all animals were positive.

While the TG on the right side showed positive results for HSV-1 in immediate infection, positive signals in the right OB were not evident in all animals until late infection. Although a slight further delay could be seen for infection of the left OB, the time frame for spread to the contralateral OB was reduced as compared to transfer from right to left TG.

Through qPCR, the selectivity of our rat model in causing HSV-1 CNS infection after nasal instillation was confirmed, as HSV-1 DNA was only found in CSF and not in serum in rats 5 days p.i. (data not shown). This indicated that despite the

**Fig. 2** Paraffin sections of olfactory region from a rat 3 days after intranasal infection with HSV-1. **a** Nasal cavity. **b** Right olfactory bulb with mitral cells (*M*). **c** Rhinal cortex (*rc*), lateral olfactory tract (*lo*). **d** Right trigeminal ganglion. Nuclei are counterstained with haematoxylin. Scale bars: 500  $\mu\text{m}$  (**a** and **c**); 100  $\mu\text{m}$  (**b** and **d**). In the early phase of infection, HSV-1 antigen (brown, stained with anti-HSV-1 antibody) could only be demonstrated in the right trigeminal ganglion (**d**)



heavy local infection in CNS, no blood-borne infection was present in the periphery.

#### Distribution of HSV-1 spread through immunohistochemistry

Tissues for immunohistochemistry were obtained from day 3 p.i. (early infection) to day 6 p.i. (late infection) and stained with antibodies against HSV-1-antigen and, when applicable, also counterstained with antibodies for different neuronal cell markers. In parallel with the findings of HSV-1 DNA by qPCR, the infection was more widespread in the brain during late infection. To identify different neuronal cell types, monoclonal antibodies were used. Neurons were identified using the neuronal nuclear marker hexaribonucleotide binding protein-3 (NeuN), astrocytes were identified as positive for glial fibrillary acidic protein (GFAP) and microglia was identified using antibodies to ionized calcium binding adaptor molecule 1 (Iba1). Although no appropriate oligodendrocyte marker was available for immunohistochemistry, we detected during the experiments that AQP9, a membrane-bound water channel also permeable for glycerol (Ishibashi et al. 1998), was extensively expressed in GFAP-negative glial cells that morphologically resembled oligodendrocytes. Even though AQP9 has been reported to be expressed by astrocytes and catecholaminergic neurons (Badaut 2010; Badaut et al. 2004, 2014; Lehmann et al. 2004), a polyclonal antibody for AQP9 was used as a marker for oligodendrocytes in the absence of positive signals for the other neuronal cell markers.

#### Early infection (3 days post-infection)

In early infection, no HSV-1 antigen could be demonstrated in the nasal mucosa or in the OBs (Fig. 2 a–c). At the same time point, however, HSV-1 antigen was detected in scattered neurons in the right TG (Fig. 2d), reflecting the findings from qPCR (Fig. 1a). No HSV-1 antigen was detected elsewhere in the brain in early infection (data not shown).

#### Late infection (4–6 days post-infection)

In late infection, HSV antigen was broadly detected in defined parts of the brain. The extent of infection varied between animals, but for all cases, the right part of the brain was most seriously affected. On sections taken from the right OB (Fig. 3a and b) of an animal on day 4 p.i., the mitral cells and the olfactory tracts were infected with HSV-1. In a section taken from the left side at the same level (Fig. 3c and d), HSV-1 immunoreactivity was evident in the olfactory tract. At this time point, however, the mitral cell layer of the left OB remained negative, which could illustrate that the virus does not reach the left OB from the initial site of infection but rather through contralateral spread.

In a section of the forebrain from a moderately infected rat 4 days p.i. (Fig. 4a), HSV-1 antigen was demonstrated in the rhinal cortex, in the right lateral olfactory tract and in the anterior part of the AC. On the right side of the rat brain, layer II of the rhinal cortex was selectively affected, while only scattered HSV-1 antigen-positive cells were seen for the rhinal

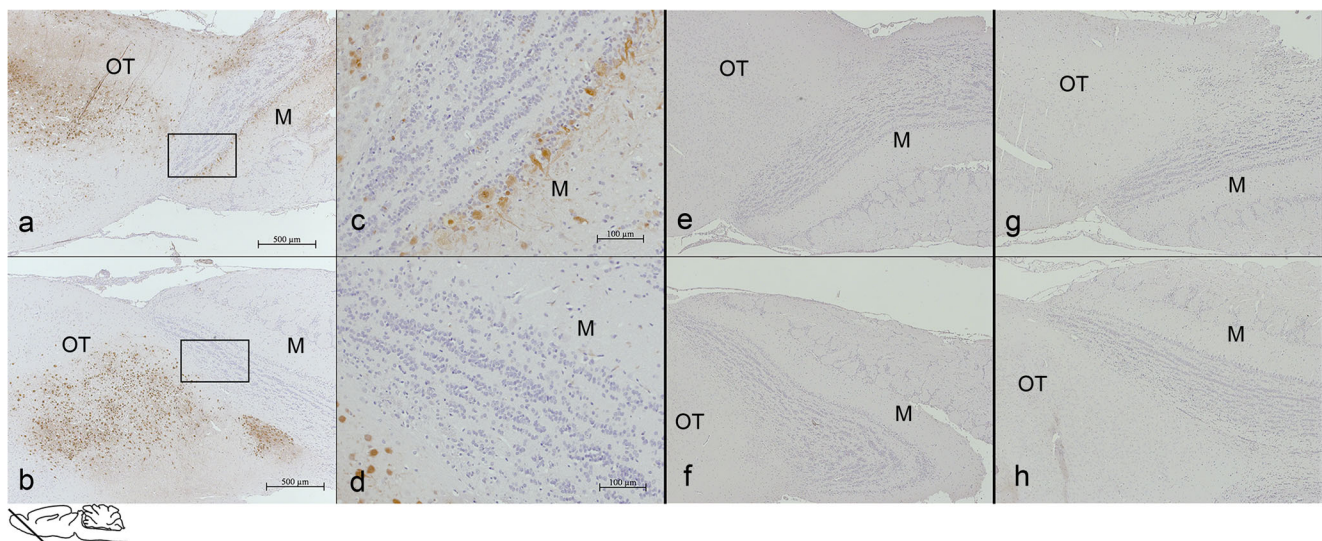


**Fig. 3** Horizontal paraffin sections of the olfactory bulbs and olfactory tracts from a rat 4 days after intranasal infection with HSV-1 (*right nostril only*). **a** Right olfactory bulb with mitral cells (*M*) and olfactory tract (*OT*). **b** Higher magnification of (**a**), with mitral cells. **c** Left olfactory bulb with mitral cells and olfactory tract. **d** Higher magnification of (**c**) with mitral cells. **e** Right olfactory bulb of infected animal incubated with control serum. **f** Left olfactory bulb of infected animal incubated with control serum. **g** Right olfactory bulb of uninfected control animal incubated with anti-HSV-1 antibody. **h** Left olfactory bulb of uninfected control animal incubated with anti-HSV-1 antibody. Nuclei are counterstained with haematoxylin. Scale bars: 500  $\mu\text{m}$  (**a** and **c**); 100  $\mu\text{m}$  (**b** and **d**). Inset indicates where in the rat brain the sections

were taken. On the *right side*, detection of HSV-1 antigen (*brown*, stained with anti-HSV-1 antibody) was evident in the mitral cells and in the lateral and intermediate olfactory tract (**a** and **b**). On the left side, cells in the olfactory tract showed HSV-1 immunoreactivity (**c**), while the mitral cells were negative (**c** and **d**). For verification of antibody specificity, sections from infected rats were either incubated with a polyclonal rabbit anti-HSV-1 antibody (**a–d**) or the control serum Dako Rabbit Immunoglobulin Fragment (**e–f**). As can be seen, HSV-1 antigen was selectively stained in (**a–d**), confirming the specificity of our antibody of choice. A section from an uninfected control animal incubated with anti-HSV-1 antibody did not present any HSV-1 antigen (**g–h**)

cortex on the left side. HSV-1 antigen was clearly present in the anterior part of the anterior commissure (*aca*) on both the right and the left side which could provide an explanation how the virus rapidly can spread from the right OB to the left OB.

In severely affected animals, as seen for a rat day 6 p.i. (Fig. 4b and c), a large number of HSV-1 antigen-positive cells were found also in the left rhinal cortex. HSV-1 antigen-positive cells were at this time point present in both the right and left arms of the AC, evident also for cases with no or minor staining in the left rhinal cortex. The AC projects nerve endings from the anterior arms to the rhinal cortex and in a severely infected animal the HSV-1 spread appeared to follow these projections from the left arm of the AC to the left rhinal cortex according to double staining experiments (Fig. 5a–d). Through double staining, it was evident that the infected cells were negative for GFAP (Fig. 5a and b).

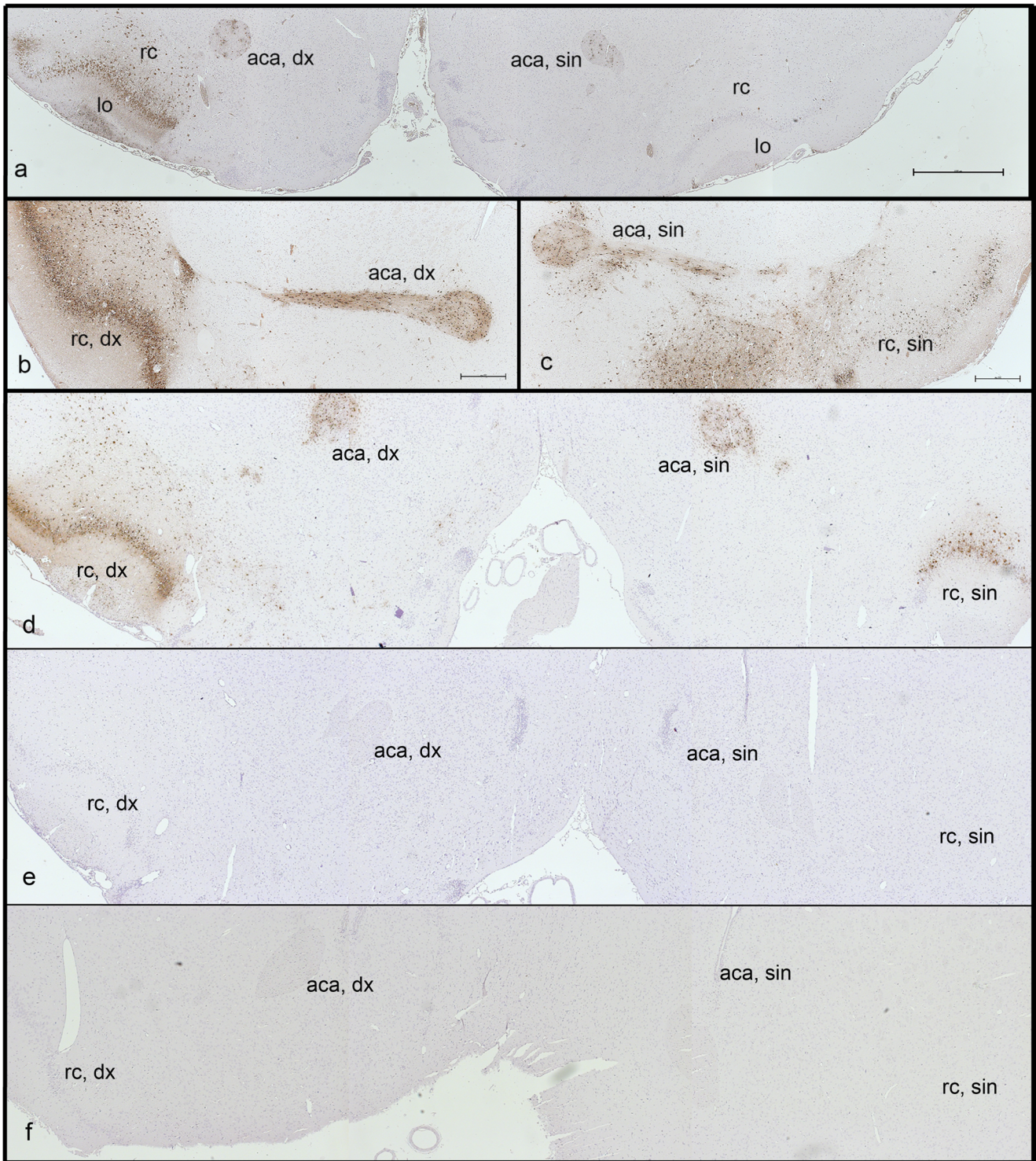
To confirm the specificity of our immunohistochemistry antibody staining, sections of the olfactory bulbs or ACs from infected rats were compared after incubation with either control serum or anti-HSV-1 antibody, where staining was only evident for the latter (Figs. 3e–f, 4d–e, 5e–f). In additional control experiments where sections of the olfactory bulbs or the ACs from uninfected animals were incubated with anti-HSV-1 antibody, no HSV-1 antigen was demonstrated (Figs. 3g–h, 4f, 5g).

**Fig. 4** Transverse paraffin section from the forebrain from rats 4 and 6 days after HSV-1 infection in the right nostril. **a** The forebrain 4 days after intranasal instillation of HSV-1 with the anterior part of the anterior commissure (*aca*) for the right (*dx*) and the left (*sin*) hemispheres, the rhinal cortices (*rc*) and the lateral olfactory tracts (*lo*). **b** Right side of the forebrain 6 days after infection with HSV-1 in the right nostril with *aca*, *dx* and the right rhinal cortex (*rc*, *dx*). **c** Left side of the forebrain 6 days after infection with HSV-1 in the right nostril with *aca*, *sin* and the left rhinal cortex (*rc*, *sin*). **d** The forebrain 5 days after infection with the *aca* and the *rc*. **e** The forebrain of an infected animal 5 days after infection incubated with control serum. **f** The forebrain of a control animal incubated with anti-HSV-1 antibody. Scale bars: 1000  $\mu\text{m}$  (**a**); 500  $\mu\text{m}$  (**b** and **c**). Inset indicates where in the rat brain the sections were taken. In a moderately infected animal 4 days after intranasal instillation (**a**), HSV-1 antigen was present in the *aca* on both sides. Many neurons in the rhinal cortex and the lateral olfactory tract on the right side showed HSV-1 immunoreactivity. On the left side, a few scattered neurons were positive for HSV-1 antigen in the rhinal cortex. Six days after infection, in a severely infected animal (**b** and **c**), there was a similar distribution of HSV-1 antigen as after 4 days, but at this late stage, the animal was more heavily infected. Slightly posterior to the plane shown in the figure, the right and left arms of the *aca* join to form the posterior part of the anterior commissure. For verification of antibody specificity, sections from infected rats were either incubated with a polyclonal rabbit anti-HSV-1 antibody (**a–d**) or the control serum Dako Rabbit Immunoglobulin Fragment (**e**). As can be seen, HSV-1 antigen was selectively stained in (**a–d**), confirming the specificity of our antibody of choice. A section from an uninfected control animal incubated with anti-HSV-1 antibody did not present any HSV-1 antigen (**f**)



Further double staining experiments gave evidence of clustering of HSV-1-positive cells in the AC (Fig. 6a), with only scattered positive cells in the immediate surrounding tissue. These cells were small and rounded with a central nucleus.

Initial experiments showed that the infected cells were negative for GFAP (Fig. 6b and c), Iba1 and NeuN, indicating that they were neither astrocytes nor microglia nor neurons. These results suggested that the HSV-1 antigen-positive cells in the



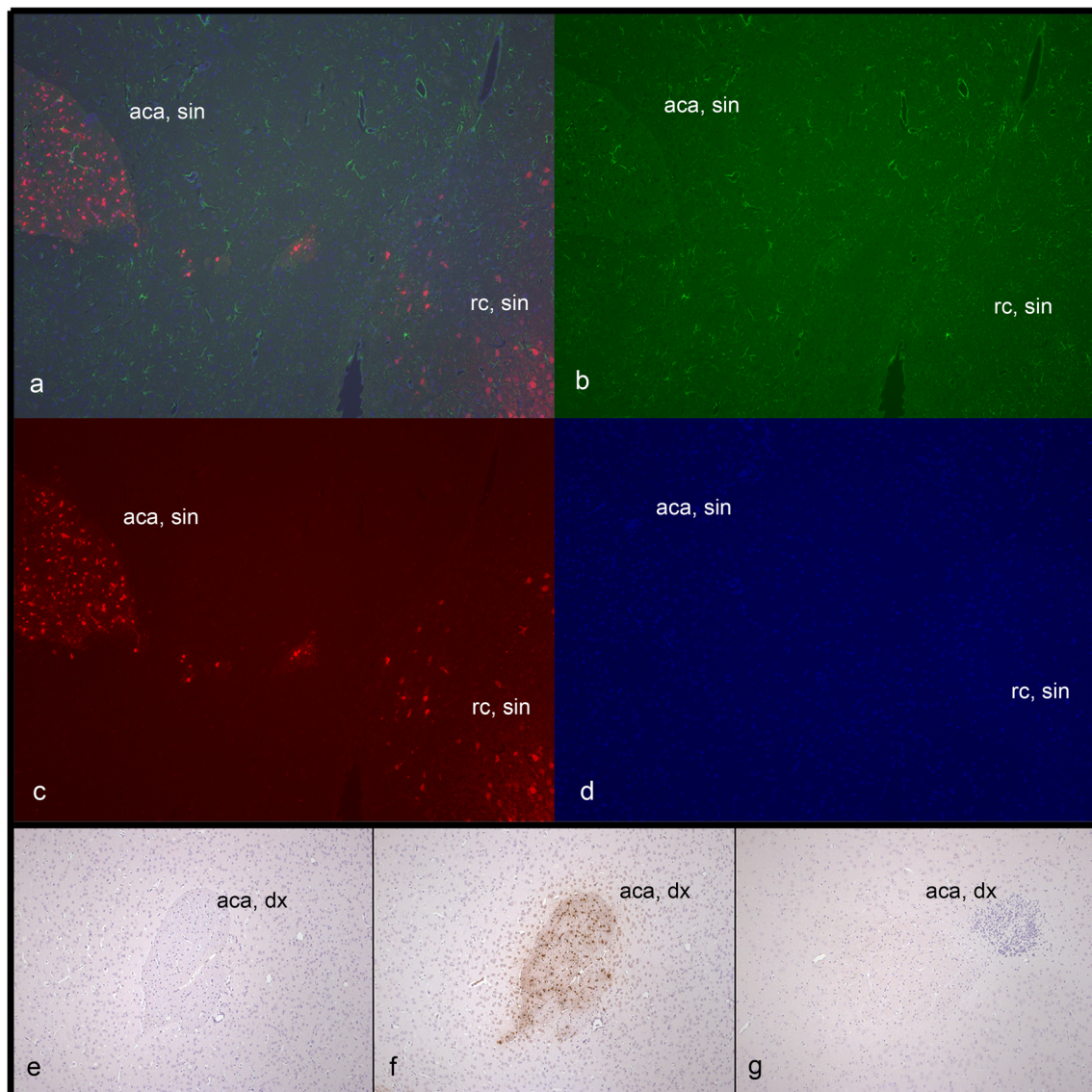


**Fig. 5** High magnification of double staining in the region of the left anterior commissure and the left lateral olfactory tract and control staining of right anterior commissure. **a** High magnification of double staining in the region of the left anterior commissure (AC) and the left lateral olfactory tract with HSV-1 antigen-positive cells in red (polyclonal antibody), GFAP-positive cells (monoclonal antibody) in green and nuclei counterstained with *Hoechst blue*. **b** Only staining for GFAP with monoclonal antibody. GFAP-positive cells (astrocytes) in green. **c** Only staining for HSV-1 with a polyclonal HSV-1 antibody. HSV-1 antigen-positive cells in red. **d** Only showing staining for nuclei with *Hoechst blue*. **e** Section of the right AC from infected rat incubated with control serum. **f** Section of the right AC from infected rat incubated with anti-HSV-1 antibody. **g** Section of the right AC from

uninfected rat incubated with anti-HSV-1 antibody. In double staining of the region around the AC, it was evident that the cells of the AC (stained for HSV-1 in red) were not astrocytes as no co-localization of GFAP and HSV-1 was seen. In (a) and (c), the staining was compatible with a spread of HSV-1 from the AC to the left rhinal cortex in bundles. To verify the specificity of our antibody staining for immunohistochemistry, sections from infected rats were either incubated with the control serum Dako Rabbit Immunoglobulin Fragment (e) or a polyclonal rabbit anti-HSV-1 antibody (f). HSV-1 antigen was selectively stained in (f), confirming the specificity of our antibody of choice. A section from an uninfected control animal incubated with anti-HSV-1 antibody did not present any HSV-1 antigen (g)

AC could be oligodendrocytes. Double staining experiments with AQP9 and HSV-1 antigen (Fig. 6d–g) indicated that HSV-1 co-localized to cells where AQP9 were expressed. As double staining with GFAP and AQP9 did not co-localize in infected cells, we interpreted the results as indicating that HSV-1-infected cells were in fact oligodendrocytes, despite previous reports of AQP9 in astrocytes.

Hippocampus was infected relatively late as compared to other structures. In cases with less severe infection, as presented in a section from an infected rat 4 days p.i., no HSV-1 antigen-positive cells could be demonstrated in the hippocampus (Fig. 7a and b). At the same time, while the rhinal cortex on the right side was infected in all cases (Fig. 7c), no infection was seen for the left rhinal cortex (Fig. 7d).

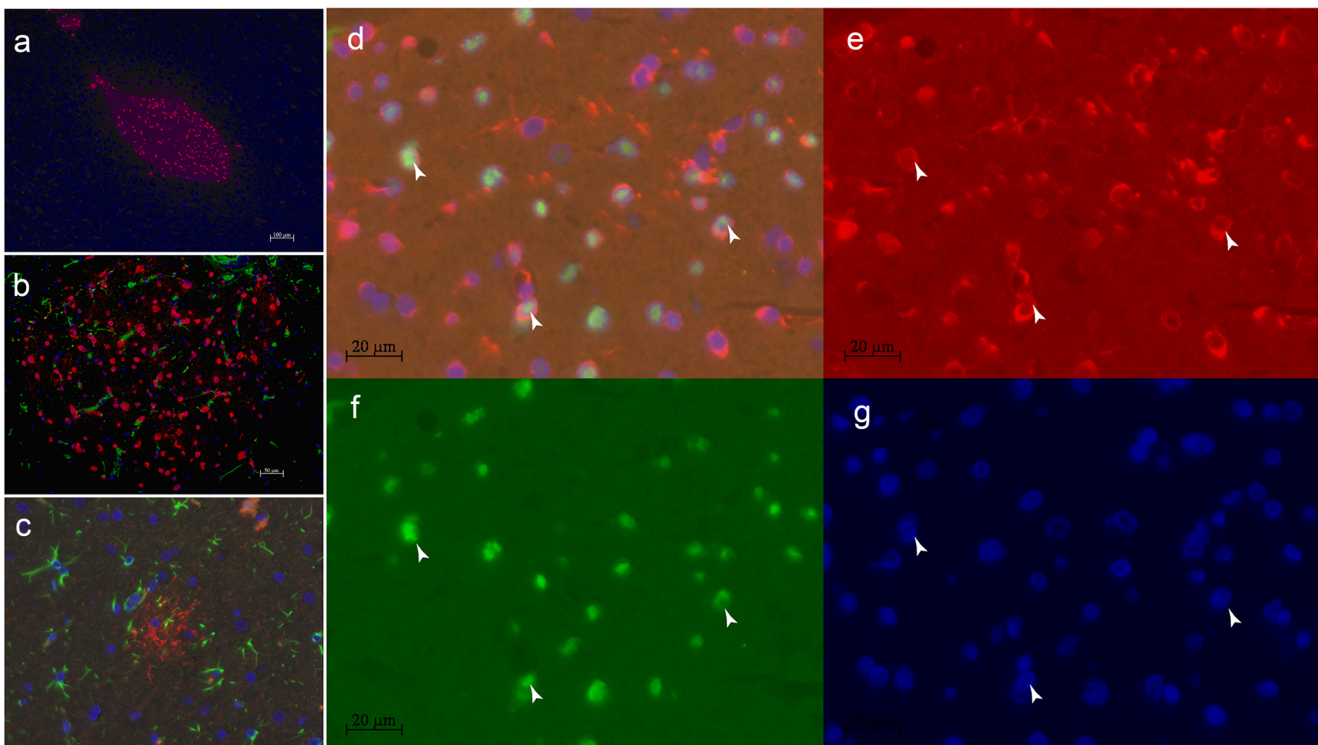


**Fig. 6** Transverse sections of the anterior commissure on the right side of a heavily infected rat 6 days after HSV-1 infection in the right nostril. **a** Anterior part of the right anterior commissure (*aca, dx*), staining in red for HSV-1 with a polyclonal antibody. **b** Higher magnification of A with double staining showing HSV-1 antigen-positive cells in red (polyclonal antibody) and GFAP-positive cells (astrocytes) in green (monoclonal antibody). **c** Double staining in higher magnification with HSV-1 antigen-positive cells in red (polyclonal antibody) and GFAP-positive cells (monoclonal antibody) in green. **d** High magnification of double staining in the anterior commissure (AC) with HSV-1 antigen-positive cells in green (monoclonal antibody), AQP9-positive cells (oligodendrocytes) in red (polyclonal antibody) and nuclei are counterstained with *Hoechst blue*. **e** Only staining for AQP9 with polyclonal antibody. AQP9 antigen-positive cells (oligodendrocytes) in

red. **f** Staining for HSV-1 with a monoclonal HSV-1 antibody. HSV-1 antigen-positive cells in green. **g** Staining for nuclei with *Hoechst blue*. Scale bars: 100  $\mu\text{m}$  (**a**); 50  $\mu\text{m}$  (**b**); 20  $\mu\text{m}$  (**d–g**). Nuclei are counterstained with *Hoechst blue* (**a–d**). Staining for HSV-1 in a severely infected animal 6 days after infection indicated that the virus had a preference for the AC (**a**). Double staining for HSV-1 with GFAP; it was evident that the astrocytes in the AC were not infected (**b** and **c**). The HSV-1-infected cells were seen as cylindrically shaped groups, with adjacent regions of astrocytes (**c**). In (**d–g**), the same section can be seen, but through different filters. This signalled for the co-localization of AQP9 and HSV-1, indicated by white arrows in all four images, and suggested that the HSV-1-infected cells of the AC were oligodendrocytes

In the later phase of infection, HSV-1 antigen-positive cells were evident in the hippocampus as well as in the rhinal cortex on both the right and the left side (Fig. 8). In the hippocampus, neurons in the CA1 region were preferentially affected (Fig. 8c and d) and the extent of injury was larger on the right side (Fig. 8c). This finding could suggest that, in addition to the TG route, the viral load derived from the right olfactory tract was decisive for the increased pathologic lesions on this side.

#### Gene expression of AQP9 in rats infected with HSV-1

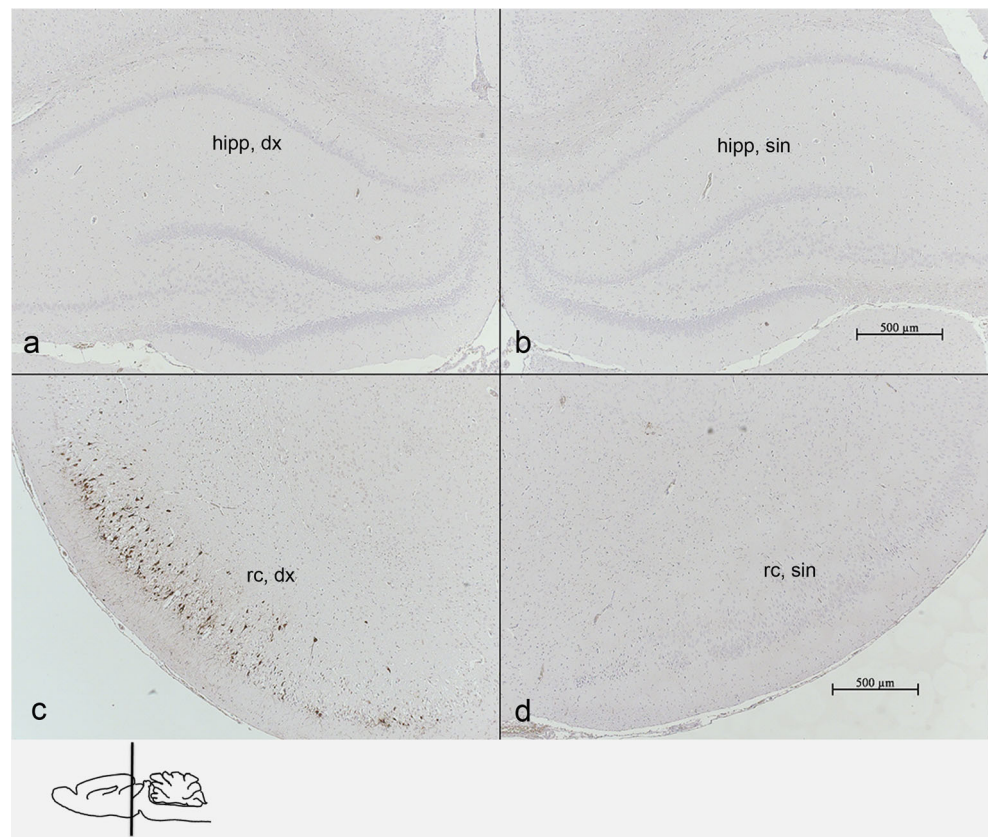
To investigate whether the AQP9 gene expression was increased during HSV-1 infection, the RNA expression of AQP9 gene was measured in rat brain tissues from HSV-1-infected rats and control rats through qPCR. Indications that the expression of AQP9 RNA was similar or higher in brain

tissue from control animals compared with infected animals (Fig. 9a) lead us to speculate that the AQP9 gene in brain cells may be constitutively expressed and unaffected by HSV-1 infection. Therefore, AQP9 protein expression could be regulated on a translational rather than on a transcriptional level. In the right AC, four out of four HSV-1-infected animals showed lower RNA concentrations than the two control animals, and similarly, this was seen for three out of four infected animals in the left AC (Fig. 9a). Hence, this could suggest messenger RNA (mRNA) consumption and AQP9 translation during initial HSV-1 infection of the brain cells.

Concentrations of AQP9 in cerebrospinal fluid (CSF) and serum samples from patients with HSE

The discovery of co-localization of AQP9 and HSV-1 in cells of the AC, the up-regulation of AQP9 in HSV-1 infected

**Fig. 7** Transverse section from the midbrain/hippocampus from a less severely infected rat 4 days after intranasal infection with HSV-1. **a** Right hippocampus (*hipp*). **b** Left hippocampus. **c** Right rhinal cortex (*rc*). **d** Left rhinal cortex. Scale bars: 500  $\mu$ m. Inset indicates where in the rat brain the sections were taken. 4 days after intranasal instillation with virus, HSV-1 antigen-positive cells were demonstrated only in the rhinal cortex on the right side (**c**). No staining of HSV-1 antigen could be detected in the hippocampus or in the left rhinal cortex



animals and indications of constitutive AQP9 gene expression lead us to investigate the expression of AQP9 in humans. CSF and serum samples obtained from HSE patients and healthy subjects were examined using an AQP9-specific ELISA kit.

The concentration of AQP9 in CSF (Fig. 9b) was statistically significantly higher ( $p=0.0073$ ), in samples from HSE patients ( $12.2\pm 4.4$  ng/ml), compared with healthy controls ( $0.0\pm 0.0$  ng/ml). For serum (Fig. 9c), the AQP9 concentration was also statistically significantly higher ( $p=0.0003$ ) for HSE patients ( $20.4\pm 1.2$  ng/ml) than for healthy subjects ( $9.2\pm 1.9$  ng/ml). Although age and sex distribution differed markedly between the two groups, and concentrations were increased in HSE patients, individual AQP9 concentrations appeared to be related to neither of these. Despite a mean age of 33.3 years for the control group compared with 62.7 years for HSE patients, a few individual subjects could be age matched with HSE patients where no age correlation could be seen for the AQP9 concentrations in serum. A 53-year-old healthy control had an AQP9 concentration of 7.33 ng/ $\mu$ l compared with an HSE patient of the same age which presented a concentration of 21.5 ng/ $\mu$ l, and a healthy subject of 56 years showed an AQP9 concentration of 8.5 ng/ $\mu$ l in serum compared with 59 years old HSE patients with concentrations of 24.2, 18.8 and 21.5 ng/ $\mu$ l, respectively. For full presentation of individual AQP9 concentrations and demographics, please refer to Supplementary Table 1. Since the mean CSF/serum

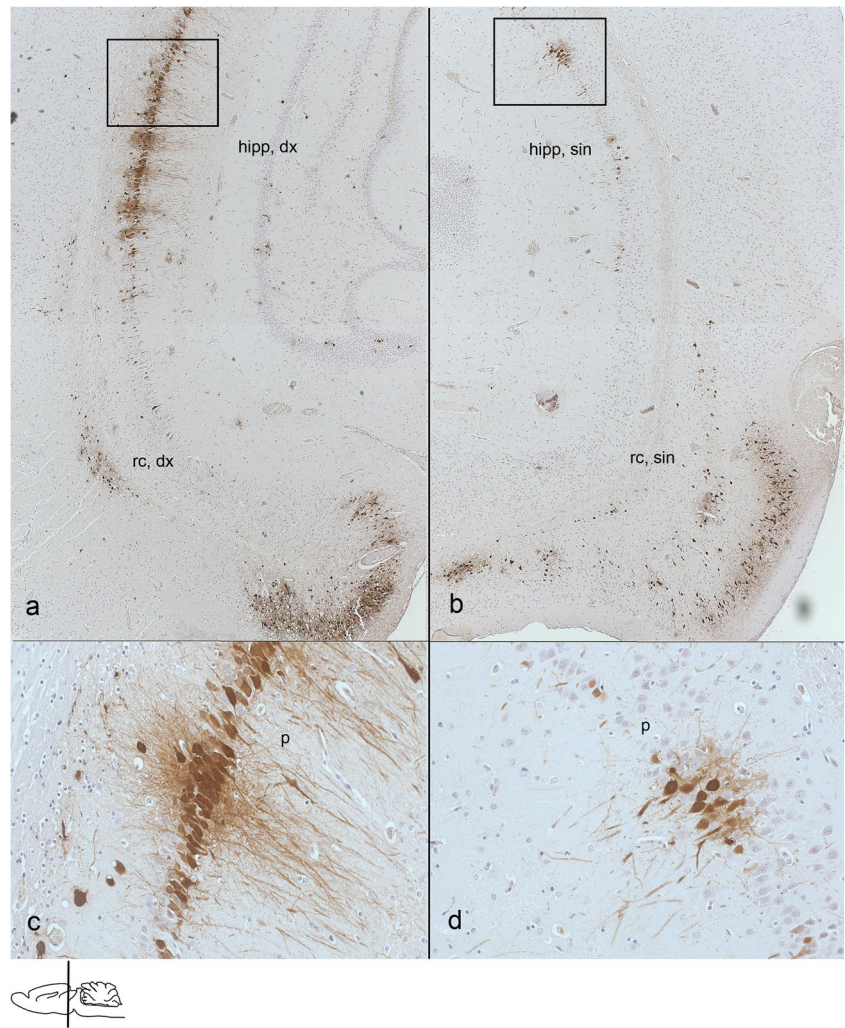
quotient of the AQP9 concentrations was more than 1/3, an intrathecal source of the protein in CSF was likely.

The concentration range of AQP9 in CSF for HSE patients could not be related to the value of genome equivalents in qPCR (median log 4.4 geq/ml, range log 3.5–log 6.3 geq/ml) nor was it gender or age specific. Although data was lacking on the duration of the infection, we found 6 patients where CSF samples were taken acute and during convalescence. Result here indicated that the concentration of AQP9 in CSF peaked early in the infection, when HSV-1 DNA concentration also was high, but late in infection (after 2 to 3 weeks) AQP9 concentration had diminished or entirely disappeared (data not shown).

## Discussion

The AC consists of bundles of nerve fibres extending from one brain hemisphere to the other, passing through either the anterior or the posterior arm, which permits communication between the two hemispheres including the two OBs. The origins for the fibres passing through the AC differ slightly for different mammalian species (Jouandet and Hartenstein 1983). In marsupials, which lack corpus callosum, the AC functions as their major interhemispherical pathway

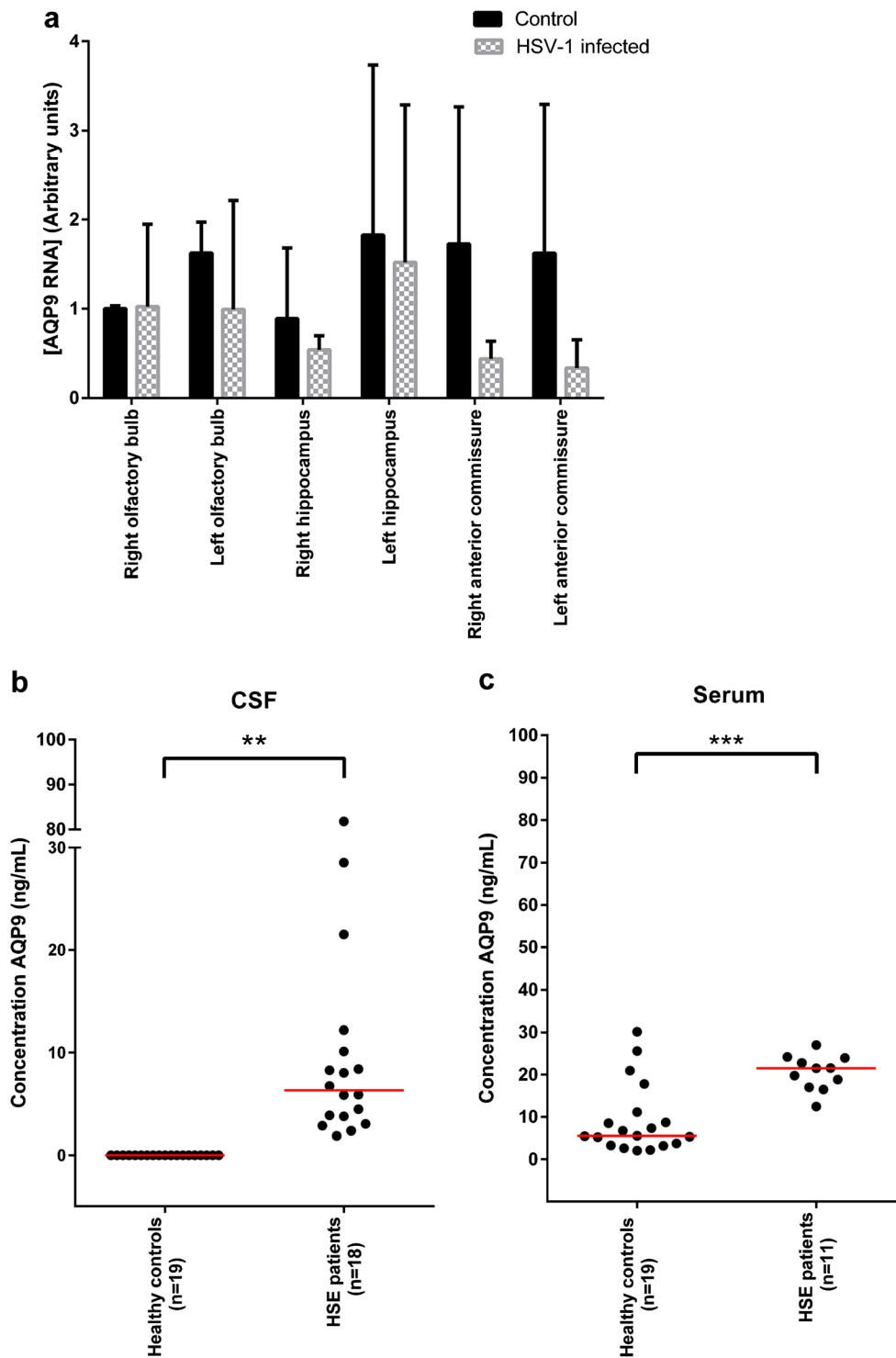
**Fig. 8** Transverse section from a severely infected rat 6 days after intranasal infection with HSV-1 **a** Right rhinal cortex (*rc, dx*) and hippocampus (*hipp, dx*). **b** Left rhinal cortex (*rc, sin*) and hippocampus (*hipp, sin*). **c** Right hippocampus with pyramidal cells (*p*). **d** Left hippocampus with pyramidal cells. Scale bars: 500  $\mu\text{m}$  (**a** and **b**); 100  $\mu\text{m}$  (**c** and **d**). Inset indicates where in the rat brain the sections were taken. HSV-1 antigen-positive cells were evident in the hippocampus and the rhinal cortex on both sides, but the lesion on the right side were more pronounced than on the left side (**a** and **b**). In the hippocampus, the pyramidal cells (*p*) in the CA1 region (the first region in the hippocampal circuit that yields a significant output pathway) were preferentially affected (**c** and **d**)



(Ashwell et al. 1996; Heath and Jones 1971), while in eutherians (including rat, mice, and primates), the AC is an important communication route reported to attribute to smelling, hearing, emotion, speech, memory and pain sensation (Risse et al. 1978). Here, fibre origins include olfactory tracts and amygdala (Di Virgilio et al. 1999; Jouandet and Hartenstein 1983; Kiernan 2012; Patel et al. 2010).

Although the anterior arm of the AC, involved in transfer of olfactory signals, is thought to be less extensively developed in humans than in rat (Di Virgilio et al. 1999; Jouandet and Hartenstein 1983; Shipley and Ennis 1996), our findings that HSV-1 uses the AC as a shortcut between the OBs in rat, as indicted through both immunohistochemistry and quantitative PCR, might be applicable to humans. The tropism for this neuronal pathway, shown to be one of the most preserved pathways in evolution, indicates that alphaherpesviruses may have developed their route for infection of the CNS early in the evolutionary chain. Through the AC, HSV-1 has utilized a robust route of connectivity to spread between the two

hemispheres with significant impact on the transmission of the HSV-1 between the OBs. As the OBs are a part of the limbic system (Eslinger et al. 1982), the quick spread between them could contribute to the selective destruction of the limbic system seen in many patients with HSE (Damasio and Van Hoesen 1985; Esiri 1982). A recent study has documented how another highly neurotropic alphaherpesvirus, equine herpesvirus 9 (EHV-9), in suckling hamsters spread from the site of inoculation, via the olfactory receptor cells, to the OBs within 48 h p.i. (El-Habashi et al. 2010). These results, despite lack of separation of infection in right or left nostrils, support our findings of HSV-1 entry and spread within CNS through both the OBs and the TGs after nasal instillation. The low dose of HSV-1 utilized in the present study, which still resulted in neuropathogenesis in rats resembling that of human HSE without damage to or violation of the nasal mucosa, argues for the use of nasal instillation as a suitable model for this human disease. Unlike what is found in HSE patients, no macrophages or accumulation of lymphocytes were seen in the infected rat brains in our study. This is presumably due



to the short duration of the infection (6 days in comparison to 2–3 weeks in HSE patients).

A few studies have previously reported on viral targeting of the AC (Barnett et al. 1993; Esiri 1982; Faber and Gebhardt 1933; Ludlow et al. 2008; Perlman et al. 1990). Both previous studies and the results we present here indicate that specific

viruses can use the AC to spread differently in the brain and result in various clinical manifestations (Barnett et al. 1993; Faber and Gebhardt 1933; Perlman et al. 1990), but no previous study has demonstrated strong presence of HSV-1 antigen in the AC. As specific viruses spread differently in the CNS, the knowledge of which cell types are infected and which

◀ **Fig. 9** Aquaporin 9 (AQP9) RNA expression in rat brain tissue and AQP9 protein concentrations in cerebrospinal fluid (CSF) and serum for healthy controls and herpes simplex encephalitis (HSE) patients. **a** Expression of AQP9 RNA in rat brain tissue for control animals and HSV-1-infected animals. Error bars indicate standard deviation. **b** AQP9 concentration in CSF of healthy controls and HSE patients in ng/ml assayed by ELISA. **c** AQP9 concentration in serum of healthy controls and HSE patients in ng/ml assayed by ELISA. Median values are indicated with red line, and each individual sample is indicated with black dot (**b** and **c**). *p* values are indicated for statistically significant differences where  $**p < 0.01$ ,  $***p < 0.001$  (**b** and **c**). The RNA expression of AQP9 in rat tissue (**a**) was examined in rat brain tissues (right and left olfactory bulb (OB), right and left hippocampus and right and left anterior commissure (AC)) obtained from two groups of rats: one uninfected control group (filled bars,  $n=2$ ) and one group infected with HSV-1 sacrificed 5 days after infection (chequered bars,  $n=4$ ). Relative mRNA levels in each sample were normalized to the reference gene 18S. RNA concentration was expressed in arbitrary units according to the formula  $2^{\Delta\Delta Ct}$ , where  $\Delta\Delta Ct = \Delta Ct_{\text{reference}} - \Delta Ct_{\text{sample}}$ , where the mean  $\Delta Ct$ -value for the right OB of the control group was used for  $\Delta Ct_{\text{reference}}$ . While the RNA expression in the OBs and the hippocampus did not present major differences between the control group and the infected group, the mean values of the AQP9 RNA expression in the ACs were markedly lower for the herpes-infected group compared with the control, although not statistically significant. The concentration of AQP9 in CSF (**b**) and serum (**c**) was determined in samples from healthy controls ( $n=19$ ) and HSE patients ( $n=20$  for CSF,  $n=12$  for serum). In cerebrospinal fluid (**b**), HSE patients presented a higher AQP9 concentration compared with healthy controls, a statistically significant difference ( $p=0.0073$ ). In serum (**c**), there was also a statistically significant increase in AQP9 concentration for HSE patients compared with healthy controls ( $p=0.0003$ )

routes they utilize can be of importance for using viruses as neuronal tracers of the CNS.

In parallel to observations by Esiri (1982) regarding the HSV-1 tropism, we found that viral antigen was more abundant in one brain hemisphere than the other initially, and although viral antigen was present in the other hemisphere as well the concentration was lower. The distribution of abundant viral antigen in the brain corresponded to the degree of pathological changes seen for the brain hemispheres, which led the author to suggest that the disease originates in one hemisphere and then spreads to the other (Esiri 1982). Hence, the neuropathological findings in human HSE is compatible with a unilateral origin of infection followed by a contralateral dispersal through neuronal tracts. Relating to our results after unilateral intranasal instillation, this is highly likely, and we suggest that the AC can be involved in such contralateral spread of HSV-1.

After instillation of HSV-1 in the right nostril, we found that the virus utilizes two routes of infection to spread in the brain. (1) For the first route, virus is internalized by the neurons in the olfactory mucosa and is transported via the glomeruli to the mitral cells within the right OB by retrograde transport (Fig. 10a), in which HSV-1 antigen can be demonstrated day 4 p.i. The virus then spreads by anterograde transport posteriorly via the right olfactory tract and the right arm of the AC, cross over to the left arm of the AC and the left

olfactory tract and travels towards the left OB (Fig. 10b). Here, however, the virus does not enter the mitral cell layer of the left OB, which might indicate that mitral cells are directionally restricted in how virus is propagated. If mitral cells only accept viral input from olfactory receptor neurons, these cells will convey anterograde transport of virus to the third order neurons in the lateral tract and block retrograde viral transfer from the lateral tract neurons. In addition, the finding is a strong indication of the selectivity of our model as regards unilateral infection, where virus does not reach the left olfactory bulb from the site of initial instillation, but rather from other parts of the brain. (2) For the second route of infection, virus may enter the brain via the right TG and infect the medulla oblongata and cerebellum (data not shown). The hippocampus is infected either from the AC, the olfactory tract or the TG (Fig. 10b).

We suggest that the cells infected with HSV-1 in the AC are oligodendrocytes, based on the morphology of the cells, the co-localization of HSV-1 and AQP9 antigen and the lack of GFAP staining. It is evident that neither nerve cells nor astrocytes are infected in the AC.

While spread to the OBs from the olfactory mucosa requires passing of a synapse, there is no similar synapse passage for spread to the ipsilateral TG. This could indicate that the delay we observed for appearance of HSV-1 infection in the right OB compared with the right TG is due to synapse passing. However, the time for passage from the right to the left OB is not delayed as much as the passage from the right to the left TG which suggests that passage over the AC is rapid. The here suggested involvement of the oligodendrocyte-resembling AQP9-positive cells of the AC could contribute to this increased speed for viral transmission across the brain hemispheres.

Our results indicate that HSV-1 in the AC showed a preference for AQP9-positive cells morphologically resembling oligodendrocytes, rather than neurons or astrocytes, which might be of value for rapid spread of the virus as one oligodendrocyte can extend its processes to more than one nerve fibre. Also, we showed HSV-1 antigen presence from the left anterior arm of the AC to the left rhinal cortex compatible with following of nerve projections, which could indicate the location of where HSV-1 passes from AQP9-positive cells to neurons of the left olfactory tract

Earlier studies of HSV-1 spread in the CNS have often investigated the involvement of astrocytes in infection (Aravalli et al. 2006; Armien et al. 2010; Studahl et al. 2000; Toft-Hansen et al. 2011). Oligodendrocytes, which are strongly permissive for HSV-1 infection (Bello-Morales et al. 2005), have rarely been in clinical focus for involvement in infection, but studies involving oligodendrocytes have indicated positive signals for HSV-1 antigen presence here

(Bergström et al. 1994; Esiri 1982; Mann et al. 1983; Thomas et al. 1991).

In previous studies, expression of AQP9 has been described in tanyocytes, catecholaminergic neurons and some astrocytes (Badaut et al. 2004, 2014; Badaut and Regli 2004; Lehmann et al. 2004; Papadopoulos and Verkman 2013) while studies on oligodendrocytes, to the best of our knowledge, are lacking. In this study, a polyclonal antibody for AQP9 was used as an oligodendrocyte marker, as we found that staining with this particular antibody in infected cells of the AC did not colocalize with markers either for astrocytes, microglia or neurons and the AQP9-positive cells morphologically resembled oligodendrocytes.

Our findings of high concentrations of AQP9 in the CSF of HSE patients indicate an importance of this aquaporin in human CNS infection by HSV-1. Brain oedema is commonly observed in HSE, and although the underlying molecular mechanisms are poorly understood, it has been suggested that there might be disturbance in the blood–brain barrier fluid regulation (Martinez Torres et al. 2007). AQP9, aquaporin 4 (AQP4) and aquaporin 1 (AQP1) are the three aquaporins currently reported to be present in the brain, and these have all been suggested to be involved in fluid balance regulation of the brain (Badaut et al. 2007; Lehmann et al. 2004). The expression of AQP9 has previously been investigated in relation to other brain trauma but never to HSE (Badaut 2010; Badaut et al. 2014; Fossdal et al. 2012; Liu et al. 2012; Oliva et al. 2011; Wang et al. 2009; Yool 2007), but this, however, has been done for AQP1 and AQP4 (Martinez Torres et al. 2007).

The up-regulation of AQP9 we found during HSV-1 infection of humans and rodents might be directly induced by the virus, but it is more probable that the response is a defence mechanism by the brain to protect the neurons. As AQP9 is an aquaglyceroporin (Badaut 2010), also permeable for glycerol and urea and thereby involved in the energy metabolism of cells, the up-regulation could be in response to the increased need of energy during an infection. It could also be an activation in response to reduce the brain swelling seen in HSE patients and in the rodent model. Another possible explanation to the finding of higher concentration of AQP9 in CSF from HSE patients compared with controls is the reports that AQP9 is expressed in leukocytes (Elkjaer et al. 2000; Ishibashi et al. 1998). As the amount of leukocytes usually is increased in CSF in patients with encephalitis, this could result in an increased concentration of AQP9 protein. Altogether, we found that oligodendrocyte-resembling cells expressed AQP9 and that the expression co-localized with HSV-1

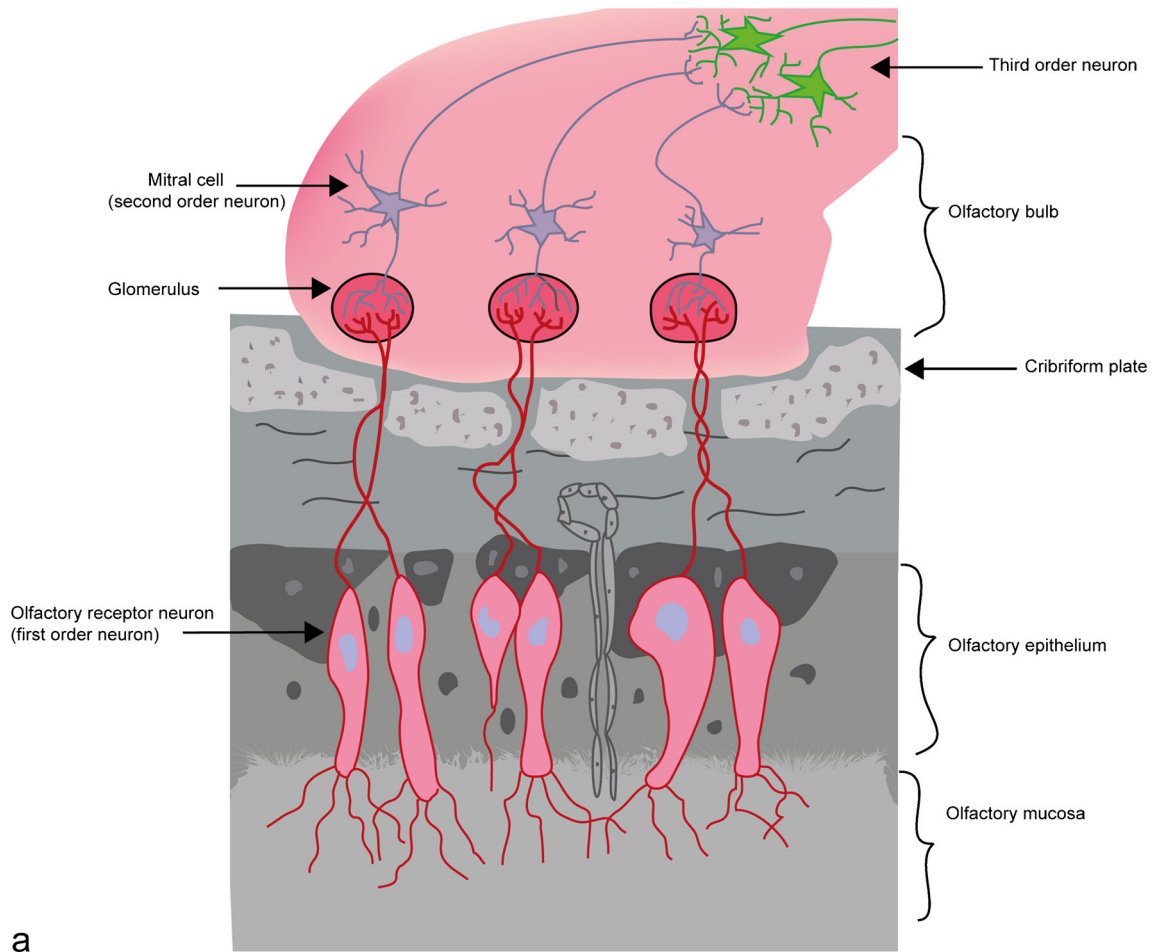
**Fig. 10** Illustration of olfactory bulb and suggested route for contralateral spread of HSV-1 CNS infection. **a** Schematic illustration of the olfactory mucosa and olfactory bulb (OB). **b** Illustration of the HSV-1 spread between the two hemispheres of the rat brain. *Solid blue lines* indicate routes for HSV-1 entry which were clearly defined during the experiments, while *dashed blue lines* indicate possible routes for spread to hippocampus and rhinal cortex. After instillation of HSV-1 in the right nostril of the rat, the virus can use two routes for entry of the brain: either through the right olfactory route (**a** and **b**) or through the right trigeminal nerve (**b**). For spread via the right olfactory route (**a**), the virus will enter via neurons of the olfactory mucosa (*first order of neurons*). Via the olfactory glomeruli HSV-1 will be transported retrogradely to the mitral cells (*second order of neurons*) of the right OB, passing the lamina cribrosa. With anterograde transport from the mitral cells to third order of neurons (**a**), the virus then can spread posteriorly (**b**) via the right olfactory tract and reach the rhinal cortex. HSV-1 can also spread from the right olfactory bulb via the anterior commissure (AC) and enter the left OB. Here, however, the mitral cells did not become infected, which could indicate that there is a blocking of viral retrograde transport of the mitral cells from the AC. Infection of the hippocampus may occur through spread either from the AC, from the olfactory tract or from the trigeminal ganglia (TGs). During spread via the right trigeminal nerve, the virus will reach the right TG and then spread further to the brain stem and medulla oblongata, the cerebellum and the left TG

antigens in experimental infection in rats, which, along with the increased protein levels detected in CSF during HSE in humans, could suggest a role for AQP9 in the pathogenesis of HSE.

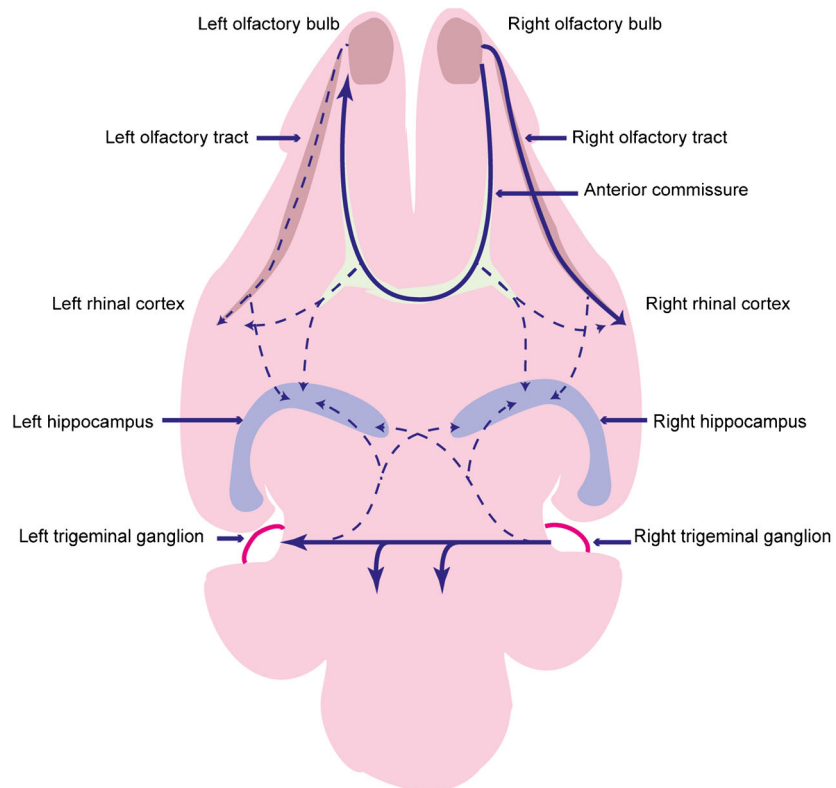
Given that our results for gene expression of AQP9 appeared to be relatively constant for both controls and virus-infected subjects, we suggest that the AQP9 gene is constitutively expressed in the brain. There may therefore be a pool of AQP9 mRNA present, and AQP9 expression could then be regulated on a translational level in brain cells in response to stress rather than on transcriptional level. In an acute event, like infection of HSV-1, the infected cells of the brain may then use the mRNA pool for translation of AQP9 protein until the production of mRNA has increased for compensation, which could explain why all infected animals showed lower RNA concentration in the right AC compared with the controls. An interesting future study could be to investigate how the expression of AQP9 mRNA is affected during the entire time course of HSE.

To conclude our results, the AC appears to play an important role in ipsi- and contralateral spread of HSV-1 in the limbic system in a rat model of HSE, which could have bearings to the appearance of clinical manifestations seen during human disease. The detection of viral antigen in AQP9-expressing oligodendrocyte-resembling cells rather than in neurons within the AC could indicate that the virus may utilize the former cell type for rapid transport. Furthermore, a role for AQP9 in the pathogenesis of human HSE was suggested by the strongly increased concentrations of this aquaporin in acute samples of CSF from patients.





a



b

**Acknowledgments** We would like to thank Maria Johansson for skilful technical assistance, Rickard Nordén and Anette Roth for technical advice and Oluf Andersen for fruitful discussions.

This work was supported by grants from the ALF Foundation at Sahlgrenska University Hospital (grant no 145–841) and the Swedish Research Council, Medicine (grant no 521-2011-3297).

**Conflict of interest** The authors declare no competing financial interests.

## References

- Aravalli RN, Hu S, Rowen TN, Gekker G, Lokensgard JR (2006) Differential apoptotic signaling in primary glial cells infected with herpes simplex virus 1. *J Neurovirol* 12:501–510
- Armién AG, Hu S, Little MR, Robinson N, Lokensgard JR, Low WC, Cheeran MC (2010) Chronic cortical and subcortical pathology with associated neurological deficits ensuing experimental herpes encephalitis. *Brain Pathol* 20:738–750
- Ashwell KW, Marotte LR, Li L, Waite PM (1996) Anterior commissure of the wallaby (*Macropus eugenii*): adult morphology and development. *J Comp Neurol* 366:478–494
- Badaut J (2010) Aquaglyceroporin 9 in brain pathologies. *Neuroscience* 168:1047–1057
- Badaut J, Regli L (2004) Distribution and possible roles of aquaporin 9 in the brain. *Neuroscience* 129:971–981
- Badaut J, Petit JM, Brunet JF, Magistretti PJ, Charriaut-Marlangue C, Regli L (2004) Distribution of Aquaporin 9 in the adult rat brain: preferential expression in catecholaminergic neurons and in glial cells. *Neuroscience* 128:27–38
- Badaut J, Brunet JF, Regli L (2007) Aquaporins in the brain: from aqueduct to “multi-duct”. *Metab Brain Dis* 22:251–263
- Badaut J, Fukuda AM, Jullienne A, Petry KG (2014) Aquaporin and brain diseases. *Biochimica et Biophysica Acta (BBA)—General Subjects* 1840:1554–1565
- Barnett EM, Cassell MD, Perlman S (1993) Two neurotropic viruses, herpes simplex virus type 1 and mouse hepatitis virus, spread along different neural pathways from the main olfactory bulb. *Neuroscience* 57:1007–1025
- Bello-Morales R, Fedetz M, Alcina A, Tabares E, Lopez-Guerrero JA (2005) High susceptibility of a human oligodendroglial cell line to herpes simplex type 1 infection. *J Neurovirol* 11:190–198
- Bergstrom T, Alestig K, Svennerholm B, Horal P, Skoldenberg B, Vahlne A (1990) Neurovirulence of herpes simplex virus types 1 and 2 isolates in diseases of the central nervous system. *Eur J Clin Microbiol Infect Dis* 9:751–757
- Bergström T, Conradi N, Hansson E, Liljeroth A, Vahlne A (1994) Resistance of rat CNS to brain stem infection with herpes simplex virus type 1. *Acta Neuropathol* 87:398–404
- Damasio AR, Van Hoesen GW (1985) The limbic system and the localisation of herpes simplex encephalitis. *J Neurol Neurosurg Psychiatry* 48:297–301
- Davis LE, Johnson RT (1979) An explanation for the localization of herpes simplex encephalitis? *Ann Neurol* 5:2–5
- De Tiege X, Rozenberg F, Heron B (2008) The spectrum of herpes simplex encephalitis in children. *Eur J Paediatr Neurol* 12:72–81
- Di Virgilio G, Clarke S, Pizzolato G, Schaffner T (1999) Cortical regions contributing to the anterior commissure in man. *Exp Brain Res* 124:1–7
- El-Habashi N, el El-Nahass S, Fukushi H, Hibi D, Sakai H, Sasseville V, Yanai T (2010) Experimental intranasal infection of equine herpesvirus 9 (EHV-9) in suckling hamsters: kinetics of viral transmission and inflammation in the nasal cavity and brain. *J Neurovirol* 16:242–248
- Elkjaer M, Vajda Z, Nejsum LN, Kwon T, Jensen UB, Amiry-Moghaddam M, Frokiaer J, Nielsen S (2000) Immunolocalization of AQP9 in liver, epididymis, testis, spleen, and brain. *Biochem Biophys Res Commun* 276:1118–1128
- Esiri MM (1982) Herpes simplex encephalitis. An immunohistological study of the distribution of viral antigen within the brain. *J Neurol Sci* 54:209–226
- Esiri MM, Tomlinson AH (1984) Herpes simplex encephalitis. Immunohistological demonstration of spread of virus via olfactory and trigeminal pathways after infection of facial skin in mice. *J Neurol Sci* 64:213–217
- Eslinger PJ, Damasio AR, Van Hoesen GW (1982) Olfactory dysfunction in man: anatomical and behavioral aspects. *Brain Cogn* 1:259–285
- Faber HK, Gebhardt LP (1933) Localizations of the virus of poliomyelitis in the central nervous system during the preparalytic period, after intranasal instillation. *The Journal of Experimental Medicine* 57:933–954
- Fossdal G, Vik-Mo EO, Sandberg C, Varghese M, Kaarbo M, Telmo E, Langmoen IA, Murrell W (2012) Aqp 9 and brain tumour stem cells. *ScientificWorldJournal* 2012:915176
- Granerod JAH, Davies NW, Clewley JP, Walsh AL, Morgan D, Cunningham R, Zuckerman M, Mutton KJ, Solomon T, Ward KN, Lunn MP, Irani SR, Vincent A, Brown DW, Crowcroft NS, UK Health Protection Agency (HPA) Aetiology of Encephalitis Study Group (2011) Causes of encephalitis and differences in their clinical presentations in England: a multicentre, population-based prospective study. *The Lancet infectious diseases* 10:835–844
- Heath CJ, Jones EG (1971) Interhemispheric pathways in the absence of a corpus callosum. An experimental study of commissural connexions in the marsupial phalanger. *J Anat* 109:253–270
- Hjalmarsson A, Blomqvist P, Skoldenberg B (2007) Herpes simplex encephalitis in Sweden, 1990–2001: incidence, morbidity, and mortality. *Clin Infect Dis* 45:875–880
- Hudson SJ, Dix RD, Streilein JW (1991) Induction of encephalitis in SJL mice by intranasal infection with herpes simplex virus type 1: a possible model of herpes simplex encephalitis in humans. *J Infect Dis* 163:720–727
- Ishibashi K, Kuwahara M, Gu Y, Tanaka Y, Marumo F, Sasaki S (1998) Cloning and functional expression of a new aquaporin (AQP9) abundantly expressed in the peripheral leukocytes permeable to water and urea, but not to glycerol. *Biochem Biophys Res Commun* 244:268–274
- Jennische E, Bergstrom T, Johansson M, Nystrom K, Tarkowski A, Hansson HA, Lange S (2008) The peptide AF-16 abolishes sickness and death at experimental encephalitis by reducing increase of intracranial pressure. *Brain Res* 1227:189–197
- Johnson RT (1964) The pathogenesis of herpes virus encephalitis I. Virus pathways to the nervous system of suckling mice demonstrated by fluorescent antibody staining. *J Exp Med* 119:343–356
- Jouandet ML, Hartenstein V (1983) Basal telencephalic origins of the anterior commissure of the rat. *Exp Brain Res* 50:183–192
- Kennedy PG, Chaudhuri A (2002) Herpes simplex encephalitis. *J Neurol Neurosurg Psychiatry* 73:237–238
- Kennedy PG, Steiner I (2013) Recent issues in herpes simplex encephalitis. *J Neurovirol* 19:346–350
- Kiernan JA (2012) Anatomy of the temporal lobe. *Epilepsy Res Treat* 2012:176157
- Kristensson K, Nennesmo L, Persson L, Lycke E (1982) Neuron to neuron transmission of herpes simplex virus. Transport of virus from skin to brainstem nuclei. *J Neurol Sci* 54:149–156
- Kuypers HG, Ugolini G (1990) Viruses as transneuronal tracers. *Trends Neurosci* 13:71–75
- Lehmann GL, Gradilone SA, Marinelli RA (2004) Aquaporin water channels in central nervous system. *Curr Neurovasc Res* 1:293–303

- Liu H, Yang M, Qiu GP, Zhuo F, Yu WH, Sun SQ, Xiu Y (2012) Aquaporin 9 in rat brain after severe traumatic brain injury. *Arq Neuropsiquiatr* 70:214–220
- Ludlow M, Duprex WP, Cosby SL, Allen IV, McQuaid S (2008) Advantages of using recombinant measles viruses expressing a fluorescent reporter gene with vibratome slice technology in experimental measles neuropathogenesis. *Neuropathol Appl Neurobiol* 34:424–434
- Mann DMA, Tinkler AM, Yates PO (1983) Neurological disease and herpes simplex virus. An immunohistochemical study. *Acta Neuropathol* 60:24–28
- Martinez Torres FJ, Volcker D, Dorner N, Lenhard T, Nielsen S, Haas J, Kiening K, Meyding-Lamade U (2007) Aquaporin 4 regulation during acute and long-term experimental Herpes simplex virus encephalitis. *J Neurovirol* 13:38–46
- McGrath N, Anderson NE, Croxson MC, Powell KF (1997) Herpes simplex encephalitis treated with acyclovir: diagnosis and long term outcome. *Journal of Neurology, Neurosurgery & Psychiatry* 63:321–326
- Misra UK, Tan CT, Kalita J (2008) Viral encephalitis and epilepsy. *Epilepsia* 49(Suppl 6):13–18
- Moon SM, Kim T, Lee EM, Kang JK, Lee SA, Choi SH (2014) Comparison of clinical manifestations, outcomes and cerebrospinal fluid findings between herpes simplex type 1 and type 2 central nervous system infections in adults. *J Med Virol* 86:1766–1771
- Mori I, Nishiyama Y, Yokochi T, Kimura Y (2005) Olfactory transmission of neurotropic viruses. *J Neurovirol* 11:129–137
- Nagashima K, Kobayashi Y, Kojima H, Hasegawa H, Kurata T (1998) Herpes encephalitis and paraneoplastic limbic encephalitis. *Neuropathology* 18:215–221
- Namvar L, Olofsson S, Bergstrom T, Lindh M (2005) Detection and typing of Herpes Simplex virus (HSV) in mucocutaneous samples by TaqMan PCR targeting a gB segment homologous for HSV types 1 and 2. *J Clin Microbiol* 43:2058–2064
- Norgren RB Jr, Lehman MN (1998) Herpes simplex virus as a transneuronal tracer. *Neurosci Biobehav Rev* 22:695–708
- Nyström K, Biller M, Grahn A, Lindh M, Larson G, Olofsson S (2004) Real time PCR for monitoring regulation of host gene expression in herpes simplex virus type 1-infected human diploid cells. *J Virol Methods* 118:83–94
- Oliva AA Jr, Kang Y, Truettner JS, Sanchez-Molano J, Furones C, Yool AJ, Atkins CM (2011) Fluid-percussion brain injury induces changes in aquaporin channel expression. *Neuroscience* 180:272–279
- Oyanguren B, Sanchez V, Gonzalez FJ, de Felipe A, Esteban L, Lopez-Sendon JL, Garcia-Barragan N, Martinez-San Millan J, Masjuan J, Corral I (2013) Limbic encephalitis: a clinical-radiological comparison between herpetic and autoimmune etiologies. *Eur J Neurol*
- Papadopoulos MC, Verkman AS (2013) Aquaporin water channels in the nervous system. *Nature reviews Neuroscience* 14:265
- Patel MD, Toussaint N, Charles-Edwards GD, Lin JP, Batchelor PG (2010) Distribution and fibre field similarity mapping of the human anterior commissure fibres by diffusion tensor imaging. *MAGMA* 23:399–408
- Perlman S, Evans G, Afifi A (1990) Effect of olfactory bulb ablation on spread of a neurotropic coronavirus into the mouse brain. *J Exp Med* 172:1127–1132
- Raschilas F, Wolff M, Delatour F, Chaffaut C, De Broucker T, Chevret S, Lebon P, Canton P, Rozenberg F (2002) Outcome of and prognostic factors for herpes simplex encephalitis in adult patients: results of a multicenter study. *Clin Infect Dis* 35:254–260
- Riancho J, Delgado-Alvarado M, Sedano MJ, Polo JM, Berciano J (2013) Herpes simplex encephalitis: clinical presentation, neurological sequelae and new prognostic factors. Ten years of experience. *Neurol Sci*
- Risse GL, LeDoux J, Springer SP, Wilson DH, Gazzaniga MS (1978) The anterior commissure in man: functional variation in a multisensory system. *Neuropsychologia* 16:23–31
- Shiple MT, Ennis M (1996) Functional organization of olfactory system. *J Neurobiol* 30:123–176
- Sili U, Kaya A, Mert A (2014). Herpes simplex virus encephalitis: Clinical manifestations, diagnosis and outcome in 106 adult patients. *J Clin Virol*.
- Skoldenberg B, Forsgren M, Alestig K, Bergstrom T, Burman L, Dahlqvist E, Forkman A, Fryden A, Lovgren K, Norlin K et al (1984) Acyclovir versus vidarabine in herpes simplex encephalitis. Randomised multicentre study in consecutive Swedish patients. *Lancet* 2:707–711
- Stahl JP, Mailles A, De Broucker T (2012) Herpes simplex encephalitis and management of acyclovir in encephalitis patients in France. *Epidemiol Infect* 140:372–381
- Steiner I (2011) Herpes simplex virus encephalitis: new infection or reactivation? *Curr Opin Neurol* 24:268–274
- Studahl M, Rosengren L, Günther G, Hagberg L (2000) Difference in pathogenesis between herpes simplex virus type 1 encephalitis and tick-borne encephalitis demonstrated by means of cerebrospinal fluid markers of glial and neuronal destruction. *J Neurol* 247:636–642
- Thomas EE, Lau AS, Kim SU, Osborne D, Kastrukoff LF (1991) Variation in resistance to herpes simplex virus type 1 of oligodendrocytes derived from inbred strains of mice. *J Gen Virol* 72(Pt 9):2051–2057
- Toft-Hansen H, Fuchtbauer L, Owens T (2011) Inhibition of reactive astrocytosis in established experimental autoimmune encephalomyelitis favors infiltration by myeloid cells over T cells and enhances severity of disease. *Glia* 59:166–176
- Turner SL, Jenkins FJ (1997) The roles of herpes simplex virus in neuroscience. *J Neurovirol* 3:110–125
- Wang H, Jin R, Tian P, Zhuo Z (2009) Enhanced expression of aquaporin-9 in rat brain edema induced by bacterial lipopolysaccharides. *J Huazhong Univ Sci Technolog Med Sci* 29:150–155
- Whitley RJ (2006) Herpes simplex encephalitis: adolescents and adults. *Antiviral Res* 71:141–148
- Whitley R, Lakeman AD, Nahmias A, Roizman B (1982) Dna restriction-enzyme analysis of herpes simplex virus isolates obtained from patients with encephalitis. *N Engl J Med* 307:1060–1062
- Whitley RJ, Alford CA, Hirsch MS, Schooley RT, Luby JP, Aoki FY, Hanley D, Nahmias AJ, Soong SJ (1986) Vidarabine versus acyclovir therapy in herpes simplex encephalitis. *N Engl J Med* 314:144–149
- Yool AJ (2007) Aquaporins: multiple roles in the central nervous system. *Neuroscientist* 13:470–485